Journal of Structural Geology 32 (2010) 1231–1249

Contents lists available at ScienceDirect

Journal of Structural Geology

journal homepage: www.elsevier.com/locate/jsg

Controls on syndepositional fracture patterns, Devonian reef complexes, Canning Basin, Western Australia

Edmund L. Frost, III *, Charles Kerans

John A. and Katherine G. Jackson School of Geosciences, Department of Geological Sciences, The University of Texas at Austin, Austin, TX 78712, USA

ARTICLE INFO

Article history:
Received 25 November 2007
Received in revised form
27 April 2009
Accepted 29 April 2009
Available online 20 May 2009

Keywords:
Syndepositional fracture
Neptunian dike
Stratigraphic architecture
P/A ratio
Canning Basin

ABSTRACT

Syndepositional fractures are an important feature of high-relief carbonate systems and exert a profound control on many facets of platform evolution and reservoir development. Based on data collected from the Canning Basin's Devonian reef complexes this study characterizes syndepositional fracture patterns as a function of variations in: lithofacies, depositional position, stratigraphic architecture, and mechanical stratigraphy. Fracture parameters, such as extension and fracture intensity, are documented to vary strongly as a function of lithofacies. The highest syndepositional extension values occurring in the microbial facies of the Famennian platform margin, with extension values three times higher than observed in equivalent Frasnian strata. Position along the depositional profile exerts a strong control on fracture patterns, with an approximate two-fold increase in syndepositional extension and fracture intensity typically observed from the platform interior to the platform margin. Syndepositional fracture intensity is shown to vary systematically with changes in platform-margin trajectory, with high fracture intensities observed in strongly progradational platforms and decreased fracture development in aggradational and retrogradational platforms. Evidence for the temporal evolution of the mechanical stratigraphy of the Devonian reef complexes is presented, with early-lithified strata effectively behaving as a single, large-scale (50–150 m) mechanical unit during syndepositional fracture development, while secondary fractures become increasingly affected by bed-scale (0.25–5 m) mechanical heterogeneity introduced by progressive diagenesis. The results presented here potentially provide a tool for predicting fracture characteristics (e.g., intensity, orientation, location, and vertical extent) from limited subsurface data and provide a method for characterizing syndepositional deformation in other systems.

1. Introduction

Large, syndepositional, opening-mode fractures, often referred to as neptunian dikes, represent an important style of deformation in many carbonate platforms throughout the geologic record. These syndepositional fractures create a laterally- and vertically-extensive, early fluid-flow system that strongly affects platform-wide diagenetic patterns (Kerans, 1985; Hurley, 1986; Whitaker and Smart, 1997; Melim and Scholle, 2002; Hunt et al., 2002; Jones and Xiao, 2006), the spatial distribution of karst enhanced permeability (Smart et al., 1988; Kosa and Hunt, 2006; Guidry et al., 2007; Baceta et al., 2007) and subsequent carbonate reservoir properties (Collins et al., 2006). Moreover, with burial or later tectonism, syndepositional fractures are often preferentially reactivated, and their distribution relative to later stress orientations can have a significant affect on ensuing deformation patterns.

Fracture development in carbonates is typically attributed to stress associated with regional tectonic deformation (Price, 1966; Nelson, 1985) or burial diagenesis (Marrett and Laubach, 2001), with fracture characteristics (e.g., spacing, orientation, and termination) ascribed to variations in bed-scale mechanical properties (Narr and Suppe, 1991; Bai and Pollard, 2000; Underwood et al., 2003; Shackleton et al., 2005). Large-scale syndepositional fracture networks present a paradox as they develop prior to significant burial and often in the absence of coeval regional deformation (Playford, 1984; Hunt and Fitchen, 1999; Kosa and Hunt, 2005). Moreover, syndepositional fractures often crosscut numerous bed-scale (0.25–5 m), "apparent" mechanical layers, implying that the mechanical units that control these features occur at the sequence to formational scale (50–150 m); a scale of mechanical stratigraphy not commonly considered in fracture studies. As a result, syndepositional fractures are typically not predicted in settings that have

* Corresponding author: ConocoPhillips Subsurface Technology, 600 N. Dairy Ashford - PR 3060, Houston, TX 77079, USA. Tel.: +1 281 293 2511.
E-mail addresses: ned.l.frost@conocophillips.com (E.L. Frost III), ckerans@mail.utexas.edu (C. Kerans).

0191-8141/$ – see front matter © 2009 Elsevier Ltd. All rights reserved.
doi:10.1016/j.jsg.2009.04.019

not experienced appreciable tectonic deformation and the enhanced vertical connectivity related to their formation is often underestimated; often leading to errant characterization of carbonate platform paragenesis and reservoir properties.

This study utilizes outcrop- and remote-sensing-scale fracture attribute data collected from the Canning Basin's Devonian reef complexes to address the following questions related to syndepositional fracture development. (1) Do syndepositional fracture patterns vary as a function lithofacies and position along a depositional profile? (2) Does a relationship exist between syndepositional fractures patterns and variations in stratigraphic architecture? (3) At what scale do mechanical units occur in early-fracture systems? And (4) do these mechanical units vary temporally with continued diagenesis?

2. Geologic setting

2.1. Regional setting

The Canning Basin is Australia's largest sedimentary basin covering approximately 430,000 km^2 and containing over 15,000 m of Ordovician- through Cretaceous-age strata (Brown et al., 1984). The Canning Basin is bounded to the east by the Proterozoic Kimberley Block and to the west by the Achaean Pilbara craton (Figs. 1 and 2). Basin development initiated in the Ordovician with broad intracratonic down-warping, followed by active rifting in the Middle Devonian through the Early Carboniferous and the development of the deeply subsiding NW–SE-oriented Fitzroy Trough (Fig. 1). Extensional values of 50% are reported within the Fitzroy Trough during the Late Devonian to Early Carboniferous (Drummond et al., 1988; Shaw et al., 1995) with the principal horizontal regional stress oriented NE–SW during the Late Devonian (Craig et al., 1984).

Throughout the Late Devonian, carbonate deposition was widespread along the eastern margin of the Canning Basin on the shallow Lennard Shelf, with the reef complexes fringing the mountainous Precambrian Kimberley Block, as well as smaller, isolated, emergent Precambrian topography (e.g., Oscar Range; Fig. 2). The 10–50 km-wide shallow Lennard Shelf is flanked to the northeast by the mountainous Precambrian King Leopold foldbelt of the Kimberley Block and to the southwest by large-scale Late Devonian extensional fault systems (e.g., Oscar Fault and Pinnacle Fault) and the Fitzroy Trough.

Two major reef-building sequences are recognized within the Devonian reef complexes, (1) the Givetian–Frasnian Pillara Sequence and (2) the Famennian Nullara Sequence (Fig. 3; Playford, 2002, and references therein). The Pillara Sequence developed during basin-wide transgression and is characterized by long-term backstepping with the development of pinnacle reefs and high-relief platforms with steep escarpment margins. Platforms of the Pillara Sequence were constructed by a consortium of stromatoporoids, corals, and calcimicrobes. Minor progradation occurred in the latest Frasnian, followed by the Frasnian/Famennian (F/F) mass extinction event and brief subaerial exposure of the reef complexes. The subsequent prograding Famennian reef complexes of the Nullara Sequence are composed primarily of high-energy grainstones with high-relief microbial margins (Hurley, 1986; Stephens and Sumner, 2003; Frost, 2007). Platform thicknesses range from approximately 300 to 600 m for the Frasnian Pillara sequence (Hurley, 1986) and 150–200 m for the Famennian Nullara Sequence (Hurley, 1986; Chow et al., 2004; Frost, 2007). Extensive early-marine cementation and microbial activity played an essential role in the evolution of both the Frasnian and Famennian reef complexes, allowing for the development of stout, wave-resistant reef rims and steep platform-margin escarpments. Early lithification also created brittle facies that were prone to syndepositional fracturing (Playford, 1980, 1984; Kerans et al., 1986).

The Devonian reef complexes were subjected to burial depths of approximately 2000 m by the Middle Carboniferous (Playford et al., 1989; Wallace et al., 1991; Frost and Kerans, 2009). During this time, the reef complexes were subjected to pressure solution, secondary fracturing, and gentle basinward tilting (Fig. 2; Hurley and Lohmann, 1989; Wallace et al., 1991). Regional uplift associated with the Alice Springs Orogeny in the late Carboniferous coupled with glaciation in the Late Carboniferous to Early Permian removed many of the younger sediments overlying the Devonian reef complexes creating a broad glacial peneplain (Figs. 2 and 4; Eyles et al., 2001; Playford, 2002), along which an extensive paleokarst network developed along Late Devonian joints and fractures within the reef complexes (Playford, 2002).

Permian glacial sediments of the Grant Group subsequently infilled much of the paleokarst network and buried the reef complexes creating a regional angular unconformity. During Permian burial, the reef complexes were again subjected to pressure solution, fracturing, and the emplacement of a second generation of blocky calcite cements (Hurley and Lohmann, 1989; Wallace et al., 1991: Fig. 2). Transpression in the Jurassic associated the breakup of Gondwana reactivated NW–SE-trending Late Devonian faults and NE–SW-trending lineaments and gently folded strata within the Fitzroy Trough (Fig. 2; Craig et al., 1984)

After broad, regional, Cenozoic uplift, the Devonian reef complexes are now represented as a rugged 350-km-long, northwest-to-southeast-trending outcrop belt of flat-topped limestone ranges. Syndepositional fractures are well exposed along the dip-oriented polished walls of present-day river gorges and along the top of most of the limestone ranges (Fig. 4).

3. Syndepositional fractures

3.1. Background and terminology

Early lithification due to marine cementation is a fundamental process in many carbonate depositional settings (Shinn, 1969; Purser, 1971; Schroder, 1973; Ginsburg and James 1976; James et al., 1976; Land and Moore, 1980; Playford, 1980; Bathurst, 1982; Harris et al., 1985; Kerans et al., 1986). In many cases early-marine cementation in carbonates is "geologically instantaneous" (e.g., months–years; Grammer et al., 1999), which allows for brittle deformation to occur shortly after deposition. In modern carbonate platforms early-marine lithification is typically extensive in the subvertical (65–90°) reef wall and steep (30–65°) upper slope (Land and Moore, 1977; James and Ginsburg, 1979), with lithified sediments reported to depths of as much as 365 m (Grammer et al., 1993). As a result, vertically-extensive syndepositional fracture networks are common in many high-relief carbonate platforms throughout the geologic record (Fischer, 1964; Playford, 1984; Smart et al., 1988; Hunt and Fitchen, 1999; Cozzi, 2000; Kosa et al., 2003; Della Porta et al., 2004; Collins et al., 2006; Guidry et al., 2007).

The Canning Basin contains one of the world's best preserved syndepositional fracture sets, and these features have been the focus of a considerable amount of research (Playford, 1980, 1984; Hurley, 1986; Kerans et al., 1986; Playford et al., 1989; Dörling et al., 1996; Ward, 1996; Miller et al., 2007; Frost, 2007; Frost and Kerans, 2009). Three primary fracture populations are recognized by this study in the Canning Basin. (1) Neptunian Dikes, well-documented, large-aperture (10 cm to 20 m), fractures filled with late Devonian marine sediment and/or radiaxial fibrous marine cement (Playford, 1984; Kerans et al., 1986; Figs. 5 and 6). (2) Syndepositional veins, smaller aperture (1 mm to 25 cm) fractures infilled with Late Devonian radiaxial fibrous, and scalenohedral marine cements

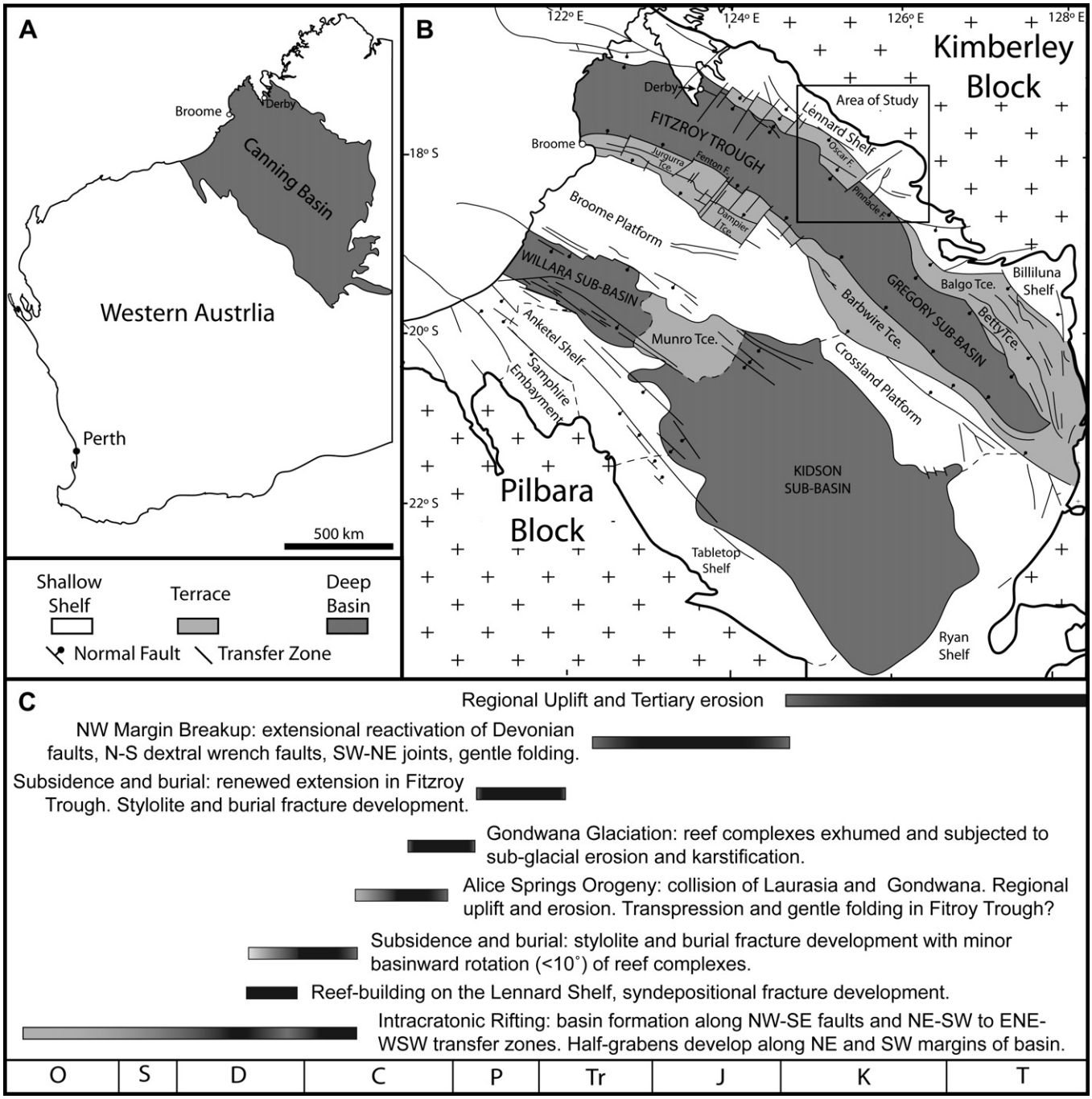

Fig. 1. Study area location and geologic setting. (A) Canning Basin location map. (B) Regional setting and structural elements of the Canning Basin, modified from Shaw et al. (1995). (C) Timing of major events impacting the Devonian reef complexes (modified from Brown et al., 1984; Craig et al., 1984; Drummond et al., 1988; Playford et al., 1989; Eyles et al., 2001).

(Kerans et al., 1986; Hurley and Lohmann, 1989), but in most cases lacking platform-top-derived sediment (Fig. 6). And (3) secondary (postdepositional) fractures with small (0.215–5 mm) apertures that are infilled with clear blocky, equant, calcite spar (Fig. 6; Hurley, 1986). Based on crosscutting relationships and isotopic data, secondary fractures are interpreted to have formed during burial in the Carboniferous and Permian (Fig. 1, Hurley and Lohmann, 1989; Wallace et al., 1991). The two syndepositional fracture populations of the Canning Basin appear to be genetically related, differing only in their degree of connection to the sea floor, and are thus collectively referred to as syndepositional fractures by this study.

3.2. Occurrence and timing

Syndepositional fractures are common throughout the Devonian reef complexes; however, they are most abundant in the early-lithified facies of the upper slope, platform margin, reef-flat (Playford, 1984), and to lesser degree, the backreef (Hurley, 1986). Syndepositional fractures in the Canning Basin are dominantly opening-mode (mode I, tensile); however, mixed-mode fractures (I/II) with a minor component of normal offset are observed in tectonically active areas (e.g., Tunnel Creek; Dörling et al., 1996; Miller et al., 2007), and in strongly prograding backreef strata (e.g., Billy Munro Gorge; Frost and Kerans, 2009). Syndepositional

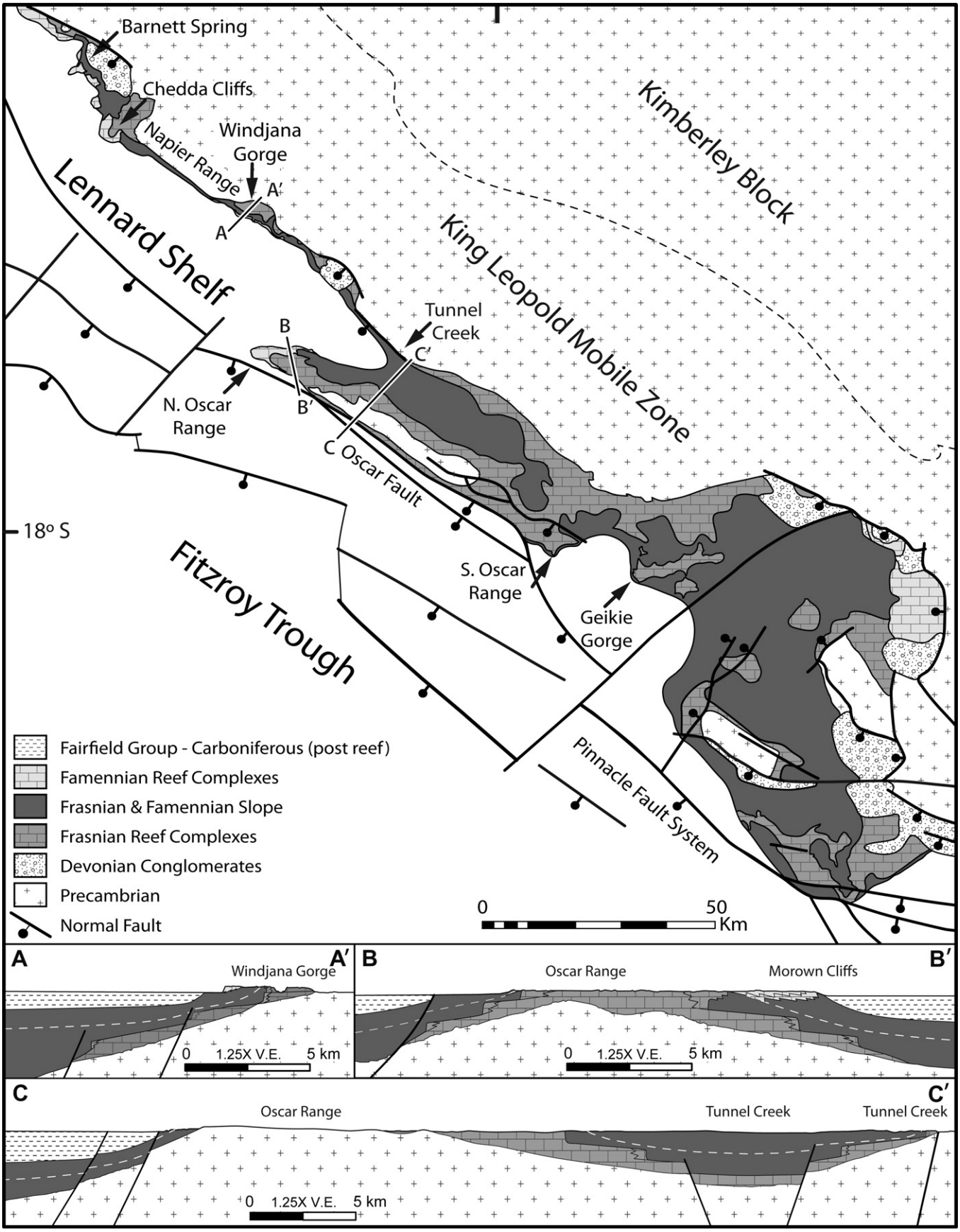

Fig. 2. Geology of the Lennard Shelf, modified after Playford and Hocking (1999).

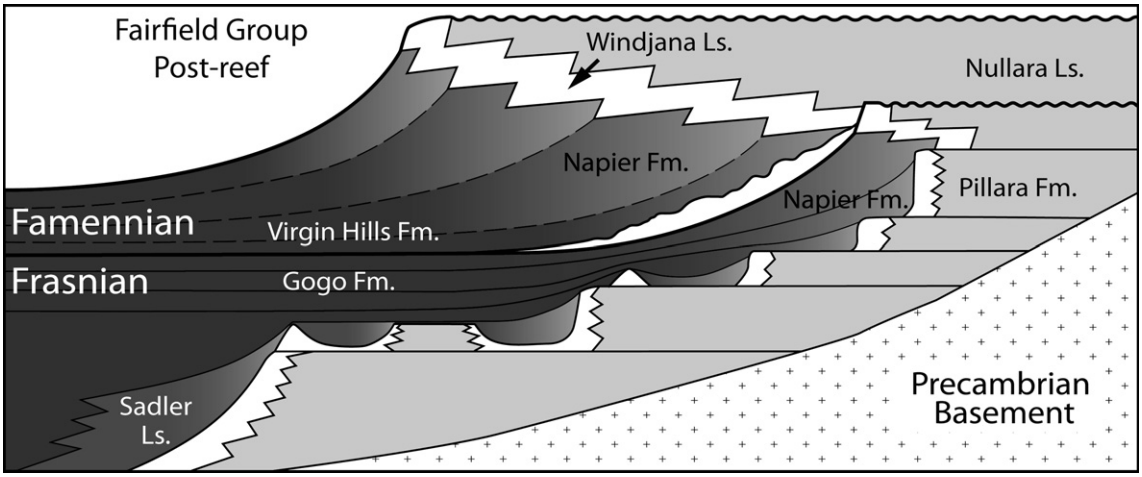

Fig. 3. Stratigraphy of the Devonian reef complexes, modified after Playford (2002).

fractures typically crosscut bedding and reach vertical heights exceeding 90 m (outcrop limit), and apertures up to 20 m and fracture trace lengths of 5 km have been reported (Figs. 4 and 5; Hurley, 1986; Kerans et al., 1986; Playford et al., 1989).

Fracture fills are highly variable (Fig. 6) and are composed of a variety of materials including: (1) marine cement; (2) microbial communities; (3) platform-top-derived detritus such as bioclastic wacke/packstones, peloidal packstones and grainstones, oolitic

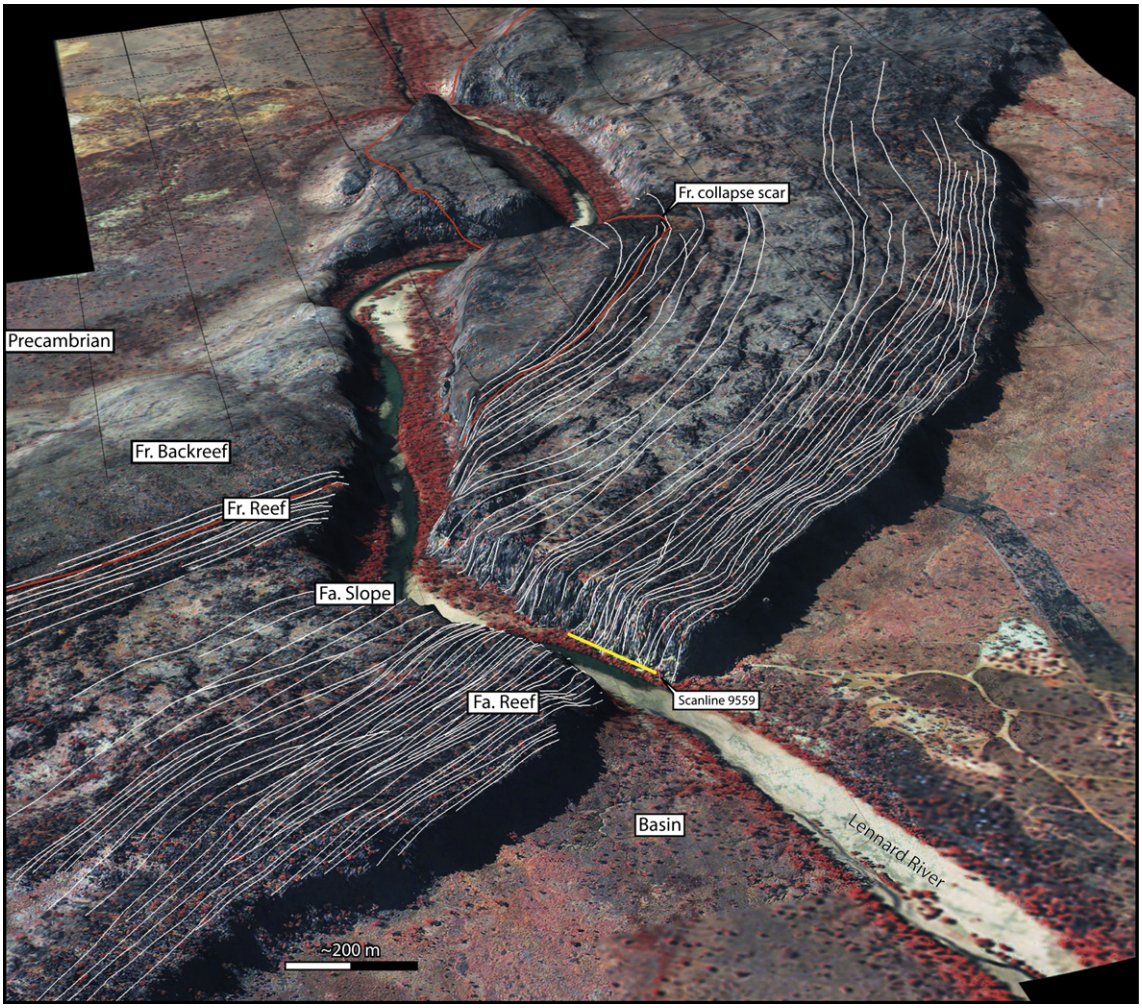

Fig. 4. Syndepositional fractures at Windjana Gorge, Napier Range. Cliff face is approximately 90–100 m tall. Image constructed from false-color IKONOS satellite imagery, high-resolution, ground-based LIDAR, and 90 m SRTM data.

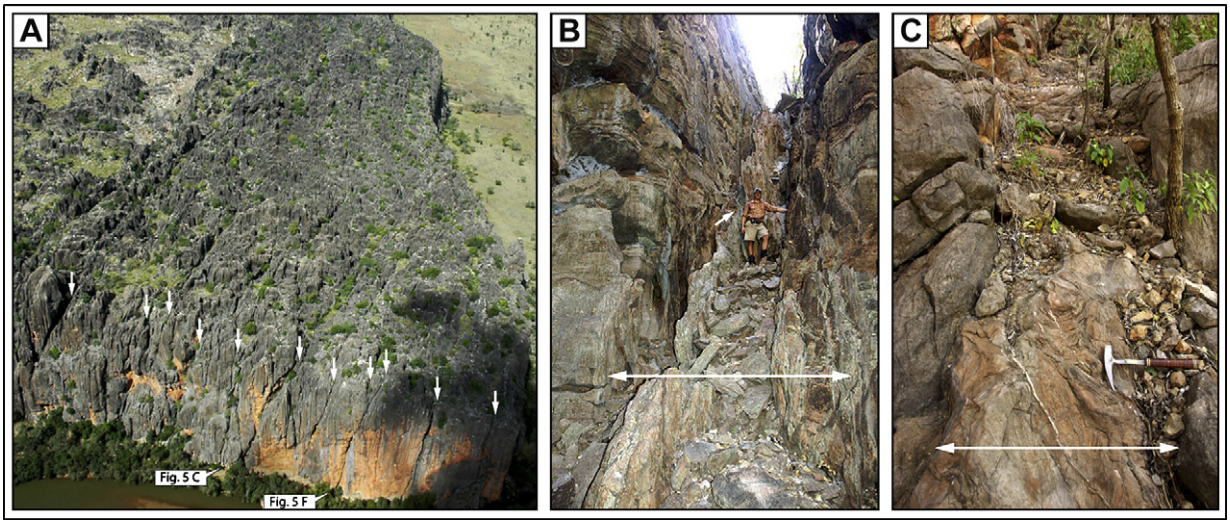

Fig. 5. Outcrop-scale syndepositional fractures. (A) Oblique aerial photo of large syndepositional fractures (white arrows) in prograding Famennian reef and forereef, Windjana Gorge. Cliff face is 90–100 m tall. Despite modern solution enhancement, a syndepositional origin is clear from fracture fill (see Fig. 6C,F). (B) Large syndepositional fracture, Famennian backreef, Billy Munro Gorge. Fracture is approximately 2 m wide and cuts through at least 65 m of backreef strata with no vertical offset. Large modern cave network has formed below field of view. Person for scale. (C) Sandstone-filled syndepositional fracture, Famennian forereef slope, Windjana Gorge. Fracture is approximately 1 m wide and cuts through at least 90 m of forereef strata with no vertical offset. Sand is horizontally laminated, implying infill from above; small crosscutting, marine-cement-lined fractures confirm syndepositional origin. Hammer provides scale.

grainstones, and siliciclastic sandstones; (4) breccia; and (5) large marine-cement-coated grains known as "spar balls" (*sensu* Playford, 1984). Fracture timing has been established as syndepositional by the recognition of: Late Devonian marine cements lining fractures; coeval platform-derived sediment and benthic organisms infilling fracture apertures; marine microbial colonies encrusting fracture walls; and by crosscutting relationships with stylolites and later fractures (Fig. 6; Playford, 1984; Kerans, 1985; Hurley and Lohmann, 1989). Secondary fractures are differentiated based on their clear, blocky, burial-phase, calcite cements (Hurley, 1986; Wallace et al., 1991), and by coeval crosscutting relationships with subhorizontal burial stylolites. Secondary fractures are strongly influenced by meter-scale bedding, and they have trace heights rarely more than a few centimeters and apertures less than 2.5 mm in width.

3.3. Controls on syndepositional fracture development

Based on previous work (Kosa et al., 2003; Guidry et al., 2007) and observations made in the Canning Basin (Playford, 1984; Hurley, 1986; Ward, 1996; Frost, 2007), Frost and Kerans (2009) proposed three basic types of drivers to generate the stress required for syndepositional fracturing (Fig. 7): (1) gravitational instability and substrate compaction; (2) differential compaction over antecedent topography; and (3) active regional tectonic deformation. Gravitational and antecedent topography controlled fractures are formed by passive deformation mechanisms intrinsic to many carbonate systems, while tectonically controlled fractures require an extrinsic mechanism such as active regional deformation. Each control type represents a unique end-member with distinct fracture patterns that can be resolved based on their orientation (Kosa et al., 2003); however, it is possible for more than one driver to be active at any given time, and care is required when interpreting the controls on syndepositional fracture development.

Gravitationally controlled syndepositional fractures are generated by extensional stress associated with (1) oversteepening and instability of the active platform-margin escarpment (Ward, 1996), and (2) down-to-the-basin tilting related to early compaction of basinal sediments and bedding-plane slippage in ductile slope strata (Hurley, 1986; Playford et al., 1989; Hunt and Fitchen, 1999). In high-relief carbonate platforms, the minimum principal stress is oriented perpendicular to the unconfined, subvertical, platform-margin escarpment (Daugherty, 1986; Whitaker and Smart, 1997), resulting in laterally-extensive, margin-parallel, opening-mode fracture networks that faithfully follow local platform-margin trends (Figs. 4, 5a and 7). Gravitational instability of the escarpment is most effective at producing fractures in the early-lithified facies proximal to the platform margin, and in the absence of any other drivers fracture intensity decreases into the platform interior. Stress associated with compaction of basinal strata (Doglioni and Goldhammer, 1988; Hunt and Fitchen, 1999; Kosa et al., 2003) and slippage along bedding planes (Playford, 1984; Hurley, 1986) also produces margin-parallel syndepositional fractures (Fig. 7). Compactional drivers are most effective in prograding platforms, where brittle early-lithified sediments build over unconsolidated slope and basin strata (Fig. 7). Once fractures are initiated in the reef facies, these features remain active as zones of weakness, which when reactivated propagate upward, and control the location of subsequent syndepositional fractures in overlying backreef strata (Kosa and Hunt, 2005).

Antecedent topography controlled syndepositional fractures are generated by differential compaction of basinal and slope strata resulting in flexure of early-cemented strata over rigid topographic elements such as older platform escarpments (Fig. 7; Hunt and Fitchen, 1999; Rusciadelli and Di Simone, 2007), forereef bioherm complexes and drowned reef spines (Frost, 2007), or crystalline basement topography (Hurley, 1986). Antecedent topography controlled fractures typically occur in swarms oriented parallel to the crest of the underlying topographic element (Hunt and Fitchen, 1999; Frost, 2007).

Tectonically controlled syndepositional fractures are defined here as fractures that are genetically related to regional faulting or folding (Nelson, 1985; Marrett and Laubach, 2001), and are orientated parallel to the active deformation feature or regional stress field (Hurley, 1986; Cozzi, 2000; Miller et al., 2007). In tectonically active areas, syndepositional fractures often occur within damage

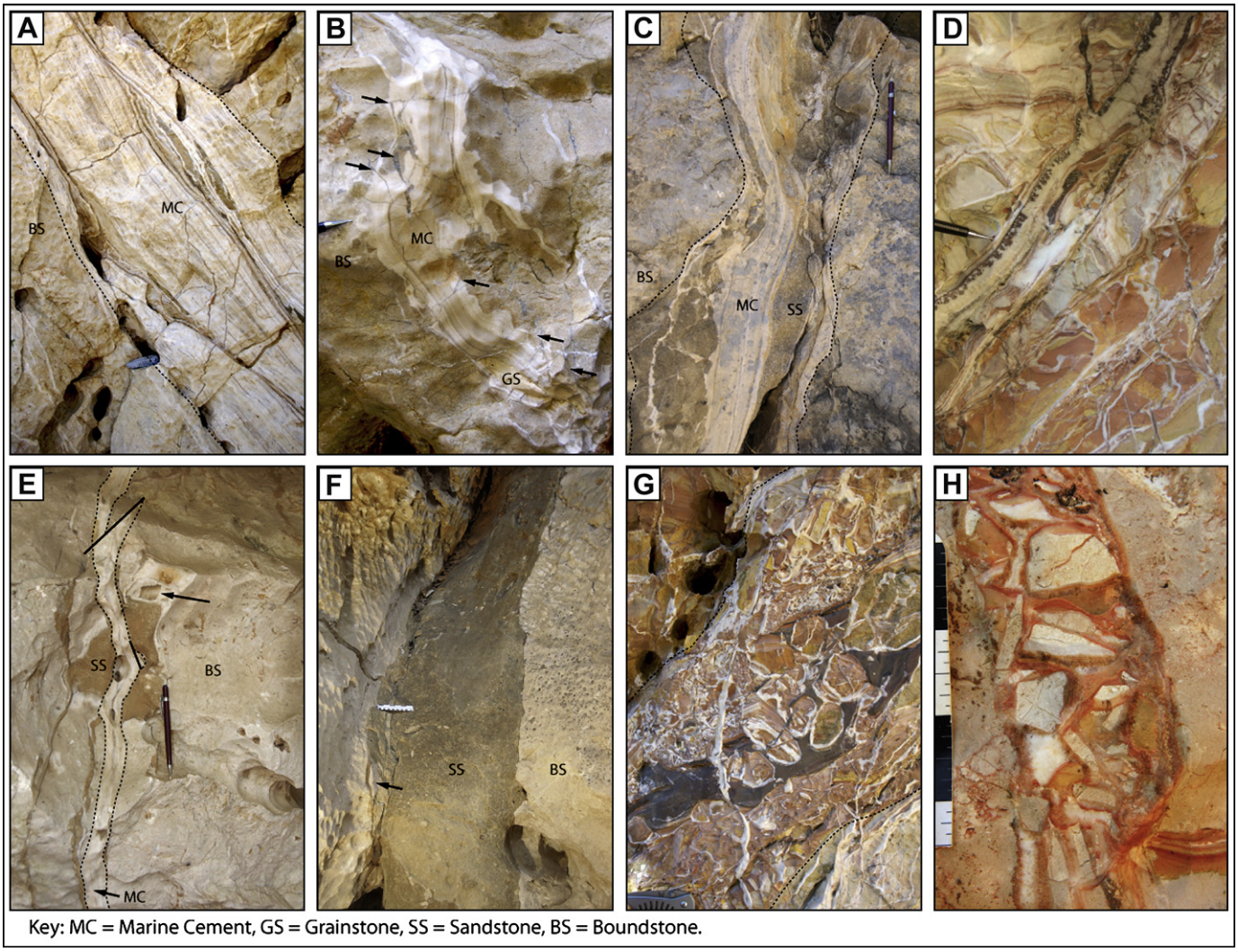

Fig. 6. Syndepositional fracture fills. (A) Marine cement in microbial boundstone, Frasnian forereef slope, Geikie Gorge. Nine-centimeter-long knife provides scale. (B) Marine cement and grainstone, with equant-spar-filled, crosscutting, secondary fractures (arrows), Famennian reefal-slope, Windjana Gorge. (C) Marine cement with sandstone, Famennian reefal-slope, Windjana Gorge. (D) Microbialite and marine cement. Frutexities colonies (dark pendant microbial growths at pen) encrust fracture wall prior to cement infill. Frasnian backreef, Tunnel Creek. (E) Sandstone and marine cement. Note ammonoid (arrow) in sandstone fill. Marine cement-lined fracture crosscuts sandstone. Famennian, reef, Windjana Gorge. (F) Sandstone and wall-rock breccia (arrows). Sandstone has same composition as (E). Famennian reef, Windjana Gorge. Scale is 15 cm long. (G) "Spar balls," marine cement, and sandstone, along minor normal fault. Frasnian backreef, Tunnel Creek. Nine-centimeter-long knife provides scale. (H) Breccia fill, Frasnian backreef, Geikie Gorge. Scale is approximately 9 cm long.

zones associated with regional faults (e.g., Geikie Gorge, Tunnel Creek, Pillara Range; Miller et al., 2007; Figs. 2 and 6).

4. Methods

In order to characterize the distribution of syndepositional fractures within the stratigraphic framework of the Devonian reef complexes, four study areas with well-exposed fractures and well-defined stratigraphy (Hurley, 1986; Ward, 1996; Playford and Hocking, 1999; Playford, 2002; Chow et al., 2004) were selected along the Napier and Oscar Ranges (Fig. 8). To test the hypothesis that syndepositional fracture characteristics (e.g., intensity and orientation) are related to lithofacies, depositional setting, and stratigraphic architecture, fracture attribute data were collected at two scales of observation: (1) platform-scale, regional lineaments with apertures of 0.5 m and larger; and (2) outcrop-scale, fractures with apertures 0.2 mm and larger.

Platform-scale fracture populations were examined for each study area on high-resolution (~1-m-pixel) IKONOS satellite imagery. Syndepositional fractures are well exposed along the top of most of the limestone ranges, with fractures often differentially weathering to form vegetation-lined corridors easily resolvable from satellite imagery (Fig. 4). Fracture traces were mapped at regional (1:24,000 and 1:10,000) and local scales (1:3309; IKONOS resolution limit). Orientation, aperture, and spacing were measured for approximately 1500 fractures ($b > \sim 0.5$ m) in 11 one-dimensional scanlines using ArcGIS (Fig. 8; Table 1). Because many syndepositional fractures are solution enhanced along the modern karst plane, aperture measurements are at best an approximation, and subsequently were not utilized to calculate extension values at the remote-sensing scale. Remote-sensing interpretations were calibrated against ground-based scanlines, field mapping, and published data (Hurley, 1986; Playford and Hocking, 1999) in order to ensure that only syndepositional fractures were recorded. The controls on syndepositional fracture development in each field area were assessed by evaluating fracture orientations relative to mapped structural elements and platform-margin trends.

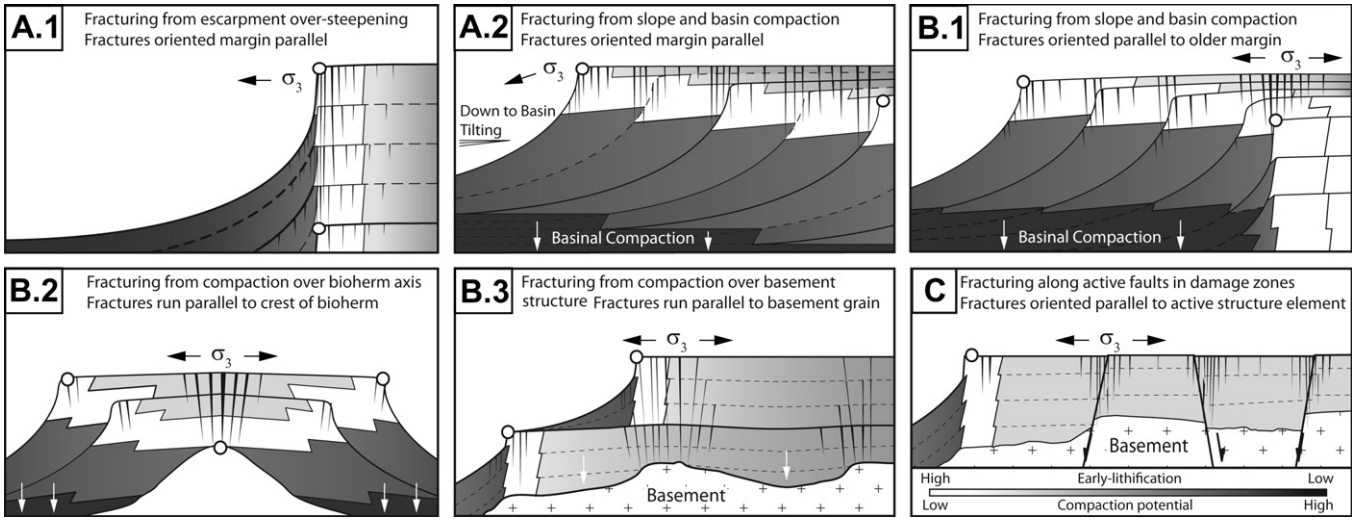

Fig. 7. Conceptual models for syndepositional fracture development. (A) Gravitational processes. (B) Antecedent topography. (C) Active regional tectonic deformation. Compiled from Hurley (1986), Playford (1984), Ward (1996), Hunt and Fitchen (1999), and Kosa et al. (2003). Modified from Frost and Kerans (2009).

Outcrop-scale fracture data were collected along the polished canyon walls of Windjana Gorge and Tunnel Creek (Figs. 2 and 4). Aperture (b) and spacing (s) were measured for approximately 1700 fractures ($b > 0.215$ mm) along 12 one-dimensional scanlines (5–134 m long) using the methodology of Ortega et al. (2006). Fracture attributes such as orientation, extension, fracture intensity, scaling, and spatial arrangement were analyzed. Syndepositional fractures were differentiated from secondary fractures on the basis of infilling and crosscutting relationships, and the fracture attributes from each population are reported separately (Table 2). In order to characterize vertical fracture relationships (i.e., crosscutting, orientation, and termination), syndepositional fracture planes were interpreted on either high-resolution (3–5 cm) ground-based LIDAR data or photomosaics and then tied to outcrop scanlines when possible.

Fracture intensity (FI; Ladeira and Price, 1981) was used to compare syndepositional fracturing at different localities, given its relative ease of acquisition at both scales of observation. FI values vary by nearly three orders of magnitude between the platform-scale (low FI) and outcrop-scale (high FI) owing to disparate resolutions of the two methods. Fracture aperture populations in each of the ground-based scanlines follow power-law scaling, allowing for large-scale apertures to be characterized from a smaller subset of fractures (Marrett et al., 1999). To facilitate direct comparison between the two scales of observation, normalized fracture intensity (FIn; Ortega et al., 2006) was calculated for apertures 0.5 m and larger (FIn0.5; roughly the smallest aperture detectable with IKONOS data) for each ground-based scanline. Results from Windjana Gorge demonstrate that FIn calculated from ground-based scanlines reasonably predicts FI calculated from remote-sensing data (e.g., 9559 and W_Fa-1; Table 1). Due to incomplete mechanical boundary preservation from modern erosion, FI was not normalized for mechanical unit thickness (*sensu* Narr and Suppe, 1991).

Progradation to aggradation (P/A) ratio quantifies platform-margin trajectory and serves as a proxy for stratigraphic architecture (Tinker, 1998; Kerans and Tinker, 1999; Della Porta et al., 2004; Frost and Kerans, 2009). P/A ratio was calculated from field mapping (this study), satellite imagery, or published data (Table 1). In the absence of a platform section, the mean thickness of age-equivalent sections was applied. Owing to differential stratigraphic preservation, aggradation values do not necessarily reflect total thickness and are best thought of as minimum values. Absolute rates are not calculated for this study because of limited chronostratigraphic data, and P/A ratios reported here represent long-term trends.

5. Large-scale syndepositional fracture patterns

5.1. Southern Oscar Range

The Frasnian outcrops of the southwest Oscar Range provide an excellent example of well-developed syndepositional fracture networks in retrograding (P/A = −2.4) and aggrading (P/A = 1.3) platforms (Hurley, 1986; Fig. 8a; Table 1). Two primary sets of syndepositional fractures in the Southern Oscar Range are recognized by this study from remote-sensing-based mapping. Set 1, weakly developed margin-parallel fractures that mimic the local morphology of the platform margin (variable trend), and set 2, fractures oriented subparallel to regional syndepositional structural features (e.g., Djowi Fault, Oscar Fault; Hurley, 1986; Playford and Hocking, 1999) with an average trend of N308°E. Set 2 fractures dominantly follow the regional structural trend of the Oscar Range (N315°E, Fig.8a), intersecting the southern margin of the Oscar Range at high angles. Based on criteria outlined in Section 4, set 1 fractures are interpreted by this study to have developed in association with gravitational instability of the platform-margin escarpment, while set 2 fractures are interpreted to be related to Devonian fault movement and differential compaction over the Precambrian antecedent basement topography (Hurley, 1986).

5.2. Northern Oscar Range

Syndepositional fractures are well exposed in the Northern Oscar Range in a series of prograding Famennian reef complexes (Fig. 8b; Table 1). Along the strongly progradational northern margin (P/A ≈ 11; Morown Cliffs, Fig. 8b), syndepositional fractures run parallel to the platform margin (N90°E), rather than the regional tectonic grain of the Oscar Range (N310°E; Playford and Hocking, 1999). In this setting Hurley (1986) reported apertures as wide as 10 m and syndepositional extension of approximately 7%. Fracture intensity values calculated for this area are among the highest observed by this study (e.g., scanline NO_Mrwn; Fig. 8b). The margin-parallel syndepositional fracture along the Morown

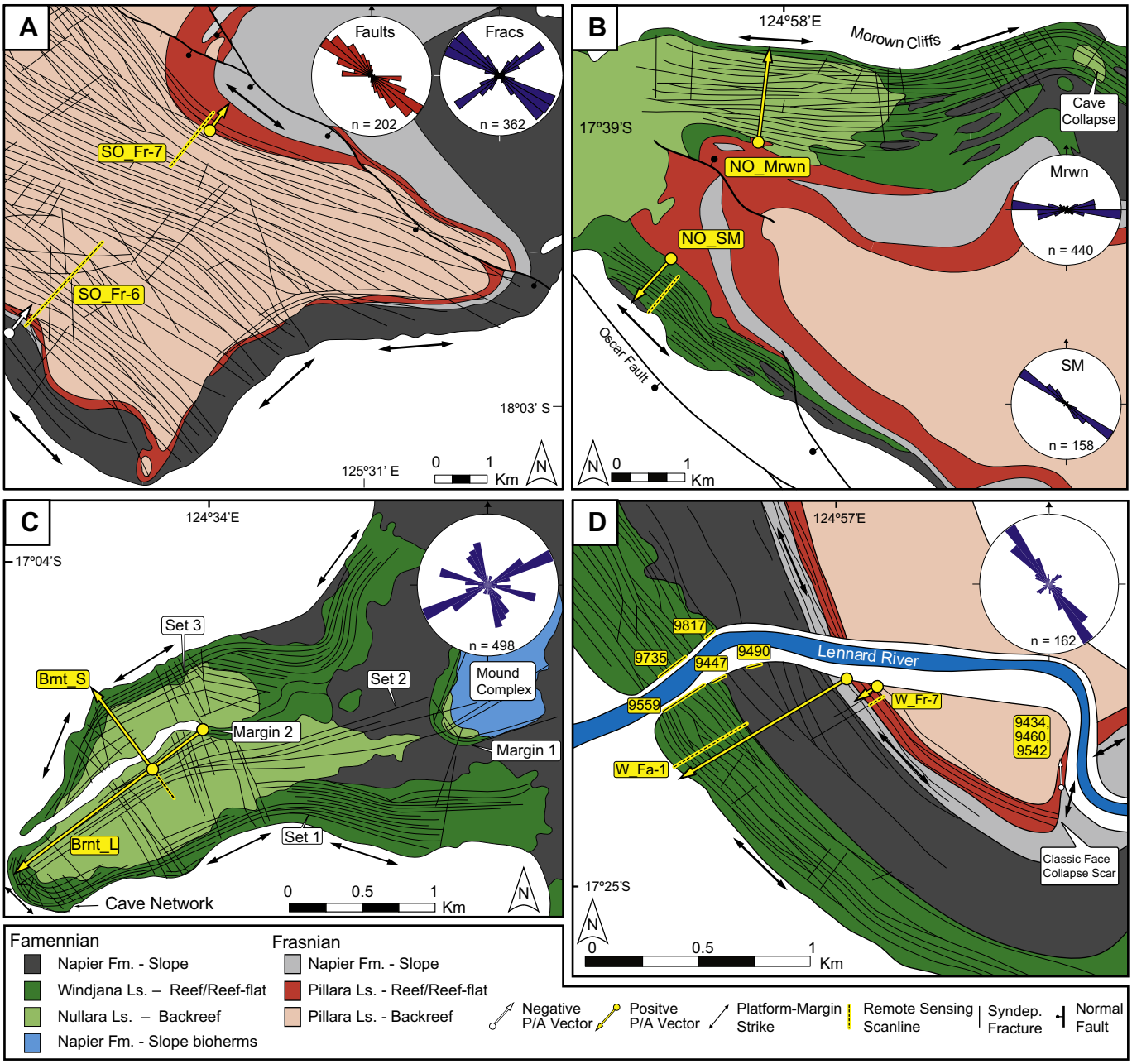

Fig. 8. Simplified fracture patterns, platform-margin vectors, and scanline locations, modified from Frost and Kerans (2009) after Playford and Hocking (1999) and Hurley (1986). Scanlines follow platform-margin vector unless otherwise noted. (A) Southern Oscar Range: syndepositional fractures dominantly follow regional syndepositional structural elements and intersect the southeast margin at high angles. Margin-parallel fractures are weakly developed and localized along SE margin. (B) Northern Oscar Range: along the Morown Cliffs, syndepositional fractures mimic platform morphology and run parallel to the margin, not regional structure. Along the southern margin, fractures also run parallel to the margin as well as the Oscar Fault. (C) Billy Munro Gorge. Three discrete syndepositional fracture sets are recognized: (1) margin-parallel fractures; (2) WSW–ENE-trending fractures that run parallel to the long axis of the platform; and (3) NNW–SSE-trending fractures that run perpendicular to the long axis of the promontory. (D) Windjana Gorge. Syndepositional fractures run parallel to the platform margin and in some instances intersect a major collapse scar at high angles.

Cliffs are interpreted to be gravitationally controlled, with compaction of forereef and basinal sediments and forereef bedding-plane slippage proposed as the dominant controls on fracture development (Hurley, 1986).

Syndepositional fractures are also well developed in the prograding Famennian reef complexes of the fault-bounded southern margin of the northern Oscar Range (Fig. 8b; Table 1). Fractures in this setting are oriented parallel to the margin (N305°E) and subparallel to the major basin-bounding Oscar fault network (N310°E). In this setting it is impossible to resolve the contributions of individual drivers in fracture formation, and, instead syndepositional fractures are interpreted to be controlled by a combination of both active regional tectonic deformation and by gravitational processes associated with progradation and margin instability.

5.3. Billy Munro Gorge

The Famennian Billy Munro Gorge platform developed as a narrow (3.5 × 1 km), highly progradational (P/A ≈ 11) promontory with a steep microbial escarpment margin (Fig. 8c; Frost and

Table 1
Fracture attributes and stratigraphic architecture data.

Scanline	Locality	Method	Control	Progradation (m)	Aggradation (m)	P/A ratio	Fracture intensity (fractures/m)		Average spacing (m)	
							Reef	Platform	Reef	Platform
Famennian platforms										
BMG_L	Billy Munro (long axis)	RS	I, II	1759	160	11.0	0.119	0.058	8.4	17.4
BMG_S	Billy Munro (short axis)	RS	I, II	685	160	4.3	0.089	0.038	11.2	26.2
MMG	Mick Malcom Gap	RS	I	1450	160	9.1	0.109	0.053	9.1	18.9
Chd	Chedda Cliffs	RS	I	1729	200[a]	8.6	0.109	ND	9.2	ND
NO_Mrwn	N Oscars (MRWN)	RS	I	1511	168[c]	9.0	0.112	0.048	8.9	20.8
NO_SM	N Oscars (SWM)	RS	I, III	550	168[c]	3.3	0.084	ND	11.9	ND
W_Fa-1	Windjana Gorge	RS	I	704	169[f]	4.1	0.088	ND	11.4	ND
9559	Windjana Gorge	G	I	613	148[f]	4.1	0.087[e]	ND	11.5	ND
Famennian platforms										
W_Fr-7	Windjana Gorge	RS	I	167[c]	233[c]	0.7	0.072	ND	13.9	ND
9434 / 9460	Windjana Gorge	G	I	−82	74	−1.1	0.051[e]	0.029[e]	16.4	34.5
SO_Fr-6	S Oscars (Fr6)	RS	III, II, I	−1326[b]	547[b]	−2.4	0.054	0.043	18.4	23.3
SO_Fr-7	S Oscars (Fr7)	RS	III, II, I	328[b]	256[b]	1.3	0.075	0.054	13.4	18.5
TC-1	Tunnel Creek	G	III, II	−100[d]	50[d]	−2.0	ND	0.074[e]	ND	13.5

Fracture intensity and average spacing for ground-based scanlines have been normalized to the minimum detectable aperture from remote-sensing data (0.5 m).
[a] Chow et al., 2004.
[b] Hurley, 1986.
[c] Playford and Hocking, 1999.
[d] Ward, 1996.
[e] Normalized fracture intensity for fractures greater than 0.50 m.
[f] Platform section absent, aggradation values based mean thickness of age equivalent sections.

Kerans, 2009). The morphology of this platform was strongly influenced by antecedent topography generated by a large series of large F-F forereef bioherm complexes (Frost, 2007). Three distinct syndepositional fracture sets are observed from remote-sensing and field mapping in the Billy Munro Gorge platform (Frost and Kerans, 2009; Fig. 8c): set 1, margin-parallel fractures; set 2, WSW–ENE-trending fractures; and set 3, WSW–ENE-trending fractures.

Syndepositional fractures of set 1 mirror the morphology of the platform margin (variable orientation) and are filled with marine-cement and platform-derived sediment, with apertures of 1.5 m or less. The highest values of fracture intensity record by this study occur in association with set 1 fractures in Billy Munro Gorge (e.g., scanline BMG_L; Table 1). Set 1 fractures are best developed proximal to the platform margin, and are interpreted to have formed in response to (A) gravitational instability of the platform-margin escarpment, and (B) compaction of basinal sediments (Frost, 2007; Frost and Kerans, 2009).

Syndepositional fractures of set 2 are oriented parallel to the long axis of the platform (WSW–ENE), and are generally restricted to a narrow swath at the center of the Billy Munro Gorge promontory (Fig. 8c). Fractures associated with set 2 have lengths in excess of 4 km and apertures up to 13 m wide (Fig. 8c) Set 3 fractures run perpendicular to the long axis of the promontory (NNW–SSE) with apertures in generally ranging from 0.5 to 2 m and lengths of up to approximately 1.5 km. Apertures of sets 2 and 3 are typically filled with platform-derived sediments (grainstone and sandstone), with minor amounts of marine cement. Set 2 fractures are interpreted to have developed from compaction of platform strata over antecedent topography of the underlying microbial mound complexes (Frost, 2007; Frost and Kerans, 2009). Set 3 fractures are interpreted to have formed from differential compaction over antecedent topography created by an older, rigid, Famennian margin (Frost, 2007; Frost and Kerans, 2009). The majority of fractures in the Billy Munro Gorge area are opening-mode; however, rare syndepositional faults with minor normal offset (<1 m) and subtle growth strata are observed by this study to occur in association set 3 basinward of an older Famennian platform margin (margin 2, Fig. 8c).

Table 2
Fracture attributes by facies.

Scanline #	Facies	Facies tract	*Syndepositional fractures*					*Secondary fractures*		
			Extension (%)	FI (fracs/m)	*FIn* (fracs/m)	S (m)	*Sn* (m)	Extension	FI (fracs/m)	S (m)
Famennian										
9559	Massive microbial bst.	Reef	9.8	16.5	0.087	0.06	11.5	1.0%	14.9	0.07
9447	Laminar microbial bst.	Reef/upper slope	9.1	11.2	0.066	0.09	15.1	1.0%	14.6	0.07
9735	Laminar microbial bst.	Reef/upper slope	7.8	8.2	0.059	0.12	16.9	1.4%	21.3	0.05
9490	Sponge–microbial bst.	Upper slope	7.0	12.1	0.055	0.08	18.2	0.8%	4.3	0.23
9817	Sponge–microbial bst.	Upper slope	5.1	10.5	0.032	0.10	31.3	0.7%	5.5	0.18
			7.8	11.7	0.060	0.09	18.60	0.98%	12.1	0.12
Frasnian										
9434	Stromatoporoid frm	Reef/reef-flat	4.0	6.8	0.061	0.15	16.4	0.1%	3.4	0.30
9539	Breccia	Fore-reef	3.9	11.1	ND	0.03	ND	ND	ND	ND
9460	Stromatoporoid flt.	Backreef	2.9	9.1	0.029	0.11	34.5	0.3%	6.1	0.16
9542	Stromatoporoid/sponge bst.	Reef/upper slope	2.8	12.6	0.030	0.08	33.3	0.7%	15.4	0.07
10500a	Stromatoporoid flt.	Backreef	1.5	1.8	0.03	0.56	33.4	0.7%	11.2	0.09
10500b	Terrigeneous pelliodal ps.	Backreef	1.4	1.8	0.03	0.57	34.1	0.2%	2.96	0.34
			2.7	7.2	0.038	0.25	29.4	0.39%	7.8	0.19

Normalized fracture intensity (FIn) and normalized spacing (Sn) were calculated for kinematic apertures of 0.5 m or larger using the methodology of Ortega et al. (2006).

5.4. Windjana Gorge

The outcrops of Windjana Gorge preserve a series of retrogradational to progradational late Frasnian to Famennian platforms (Playford, 2002; Fig. 8d; Table 1). In the retrogradational Frasnian succession (P/A ≈ −1.1) syndepositional fractures are best developed in the early-lithified strata of the reefal-slope, reef, and reef-flat and decrease in frequency into the backreef (Fig. 9; Playford, 2002; Frost, 2007). In general, Frasnian syndepositional fractures are oriented parallel to the platform margin; however, in areas where the platform margin has collapsed fractures often intersect the margin at high angles along collapse scars (Figs. 4, 8d and 9; Ward, 1996). Syndepositional fractures in the Frasnian platforms of Windjana Gorge have a vertical extent of upwards of 40 m, terminating at cycle set and sequence boundaries (Fig. 9). Given the absence of any known syndepositional fault systems in the area, it is inferred that Frasnian syndepositional fractures in Windjana Gorge formed in response to gravitational instability associated with oversteepening of the platform margin (Ward, 1996; Frost and Kerans, 2009).

The Famennian succession of Windjana Gorge is characterized by a series of progradational (P/A ≈ 4.1), microbially-constructed, grain-dominated platforms (Playford, 1984; Kerans, 1985). Although erosion associated with Permian glaciation has removed the backreef section of the Famennian reef complexes, syndepositional fracture populations in the lower reef, reefal-slope and upper forereef slope remain extremely well preserved (Figs. 4 and 5a). Syndepositional fracturing is extensive in these facies (e.g., scanlines W_Fa-1 and 9559, Table 1), with fractures oriented parallel to the platform margin, dipping either steeply toward the platform interior or with subvertical traces (70–90°). Large-scale syndepositional fractures extend for several kilometers across the top of the range (Fig. 4) and often crosscut the entire exposed Famennian section (80–100 m). Syndepositional fracture development in the Famennian of Windjana Gorge is interpreted to be gravitationally controlled (Ward, 1996; Frost and Kerans, 2009).

6. Facies control on fracture patterns

6.1. Fracture patterns in Frasnian facies

In the retrograding and aggrading Frasnian platforms of Windjana Gorge, syndepositional fractures are observed from backreef to forereef strata (Table 2; Figs. 9 and 10). The largest amounts of syndepositional extension are observed in the microbial–stromatoporoid boundstones of the reef-flat (4.0%, scanline 9434; Table 2; Fig. 10a). The Frasnian reef-flat is dominated by a series closely-spaced, large-aperture, fractures ($b > 20$ cm), with a limited number of small aperture fractures ($b < 1$ cm). Extension, aperture, and fracture intensity decrease away from the platform margin into the platform interior (e.g., scanlines 10500a/b, 9460; Table 2), as well as into the forereef slope (e.g., scanlines 9542, 9539; Table 2).

In the Frasnian reef-flat and backreef syndepositional fractures crosscut numerous and significant, bedding and lithologic boundaries, and often reach heights upwards of 40 m (Fig. 9). Paired scanlines from an early-lithified stromatoporoid biostrome bed and

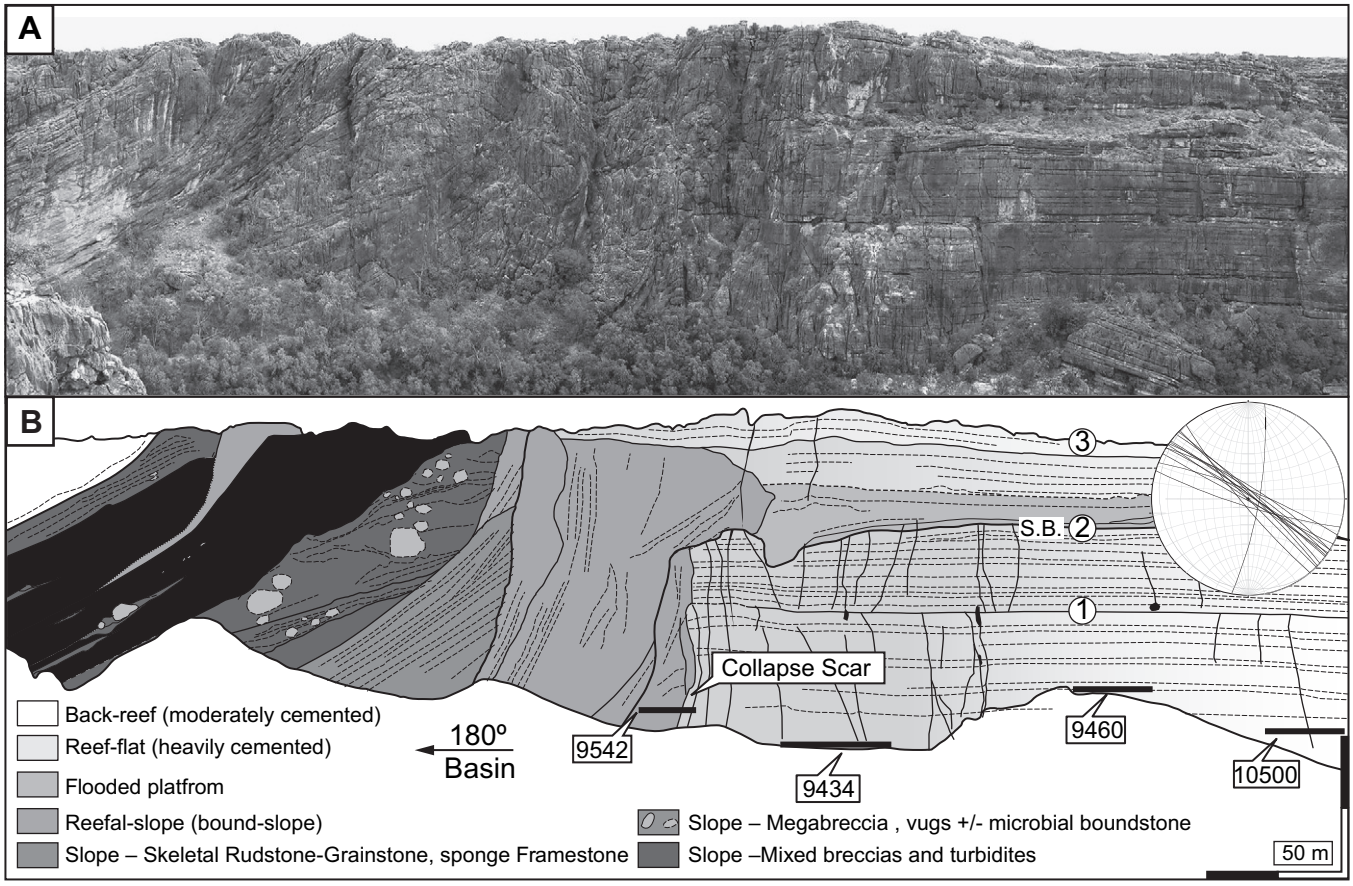

Fig. 9. Outcrop-scale Frasnian fracture patterns. (A) Photomosaic of Frasnian forereef to backreef strata, in the "classic face" (Playford et al., 1989), Windjana Gorge. Solution enhanced fractures are interpreted to be syndepositional in origin, and have been verified as such, where accessible. Three large-scale mechanical units are observed in the 'classic face" (1–3), with fractures appearing to terminate at the boundaries of these units. (B) Facies architecture, scanline locations, mechanical layers, and fracture orientation data from the "classic face". See Fig. 8d for location.

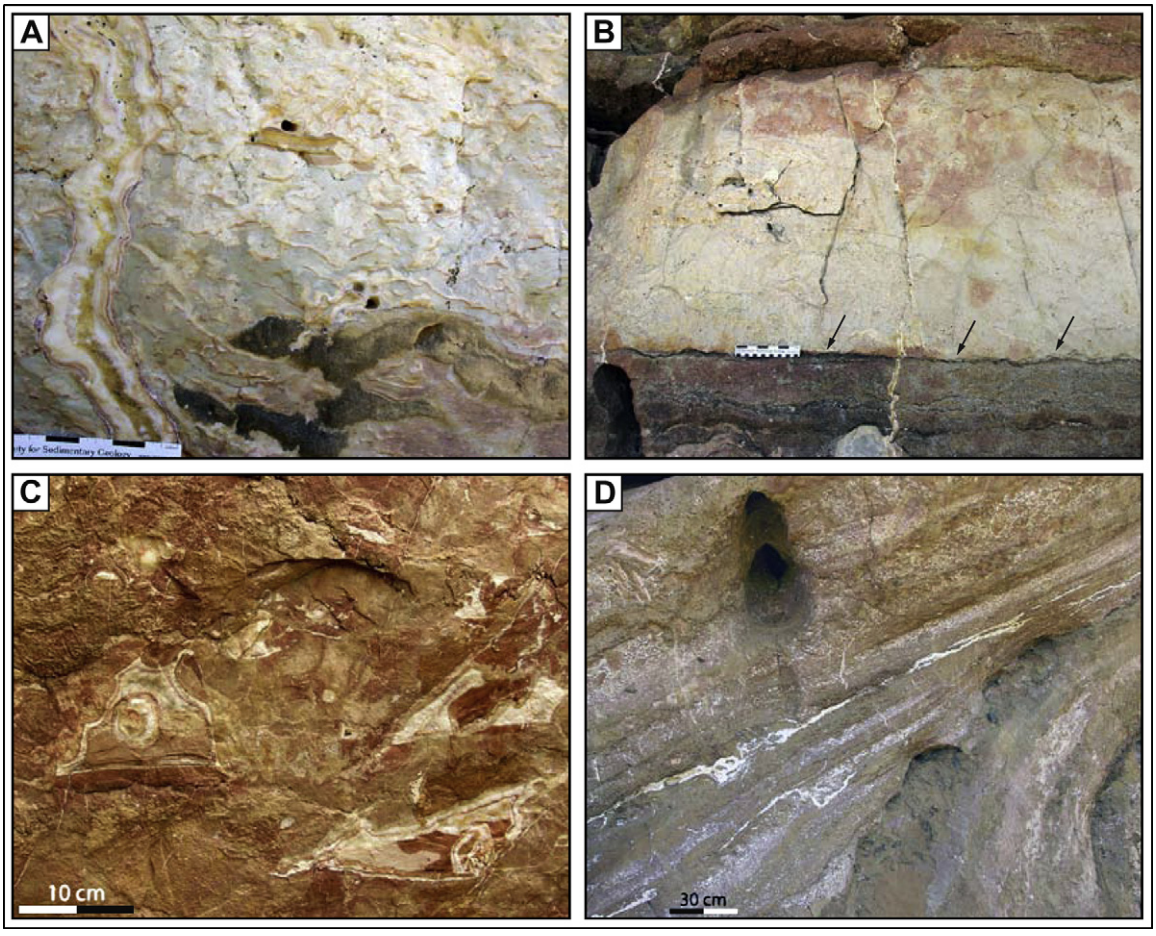

Fig. 10. Fracture patterns in Frasnian facies, Windjana Gorge. (A) Reef-flat, scanline 9434, "classic face". Marine-cement- and dolomite-lined syndepositional fracture, microbial–stromatoporoid boundstone. (B) Backreef strata, with alternating stromatoporoid biostromes (light gray) and stromatolitic, sandstone beds (dark beds); scanline 10500, "classic face". (C) Reefal-slope; scanline 9542, "classic face". Small syndepositional fractures (<5 mm) in sponge boundstone. (D) Syndepositional fractures in steeply-dipping forereef breccia, scanline 9539, east entrance of Windjana Gorge. Fractures often terminate in bedding-parallel fractures referred to as "neptunian sills" (Playford, 1984).

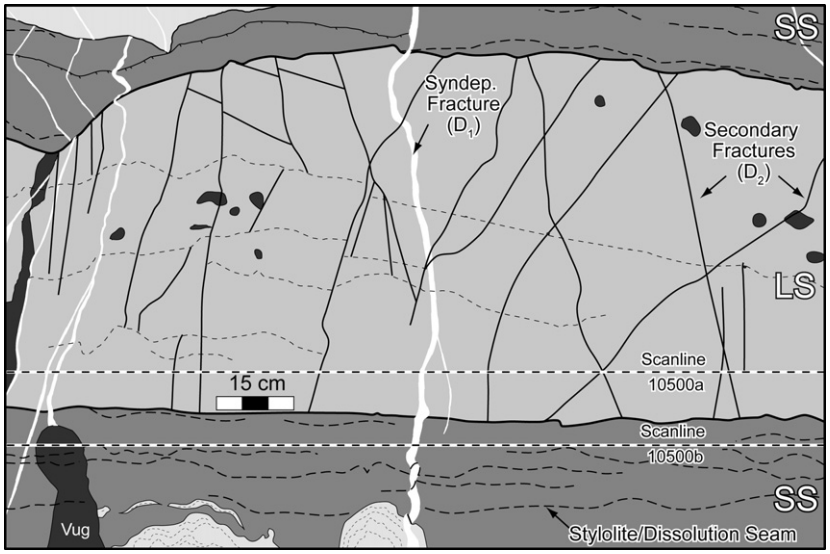

Fig. 11. Fracture patterns in Frasnian backreef, Windjana Gorge. Small syndepositional (5–20 mm) fractures are equally developed in both stromatoporoid boundstone (light gray) and stromatolitic sandstone (dark beds). Syndepositional fractures crosscut all layers and are ptygmaticly folded in sandstone beds, suggesting early compaction. Secondary fractures are well developed in biostrome facies ($S = 0.09$ m) and to a lesser degree in the sandstone beds ($S = 0.34$ m, scanline 10500b), and the majority of these fractures terminate at bedding boundaries.

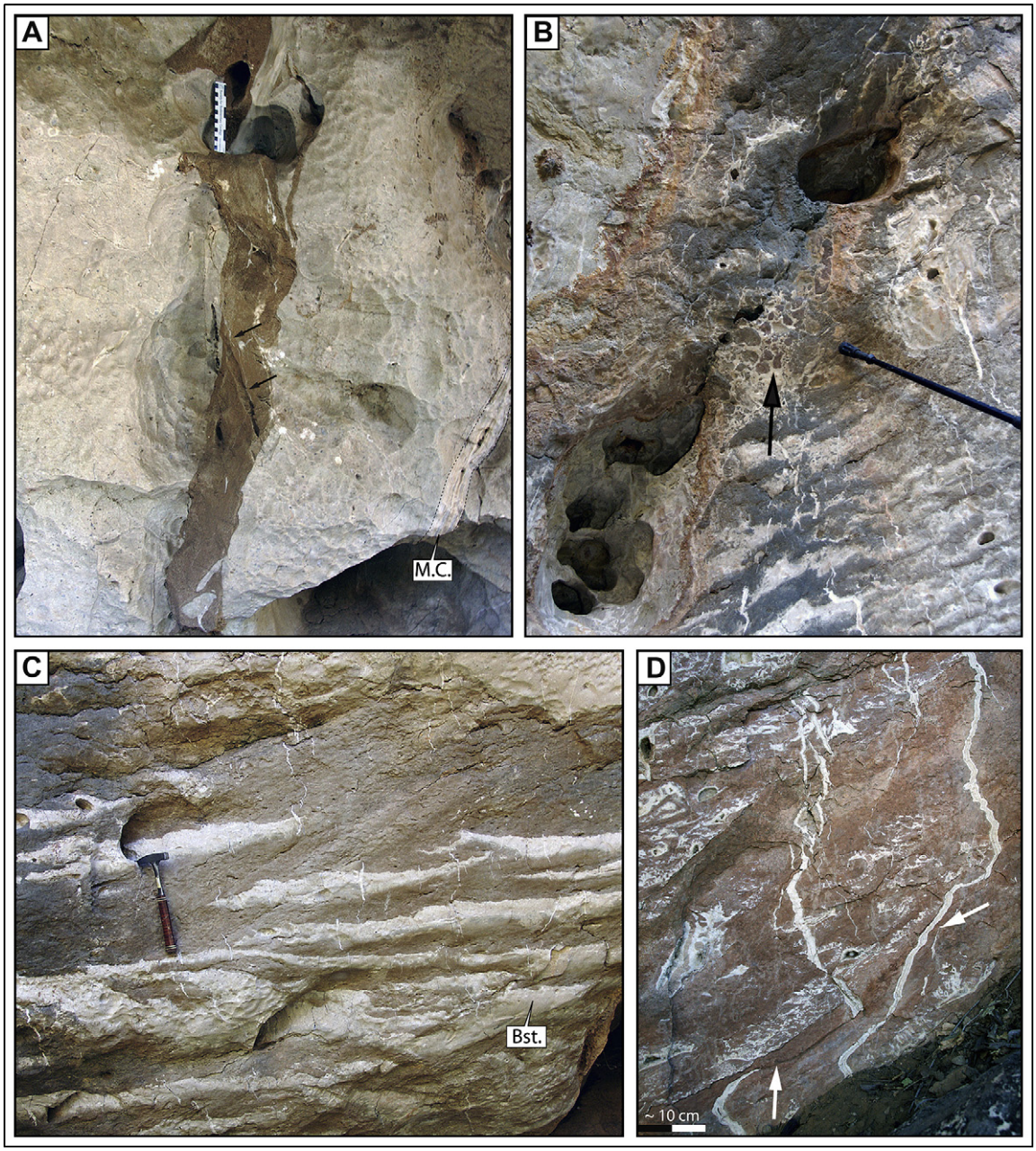

Fig. 12. Fracture patterns in Famennian facies, Windjana Gorge. (A) Sand- and marine-cement (MC)-filled fractures developed in massive microbial reef boundstone, scanline 9559. Marine cement-lined fractures (arrows) crosscut sand-filled fracture. (B) Small-scale basinward-dipping fault with spar balls developed along fault plane (arrow), in laminar microbial boundstone, north wall. (C) Laminar microbial boundstone (BS), deep reef–reefal-slope, scanline 9735. (D) Syndepositional fractures in steeply dipping (30–35°) sponge boundstone, upper bound slope, scanline 9817. Apparent down-dip slippage along bedding planes (arrows).

an overlying stromatolitic sandstone bed indicate that early fractures are equally well developed in both facies with consistent values of extension and fracture intensity observed in each bed (e.g., scanlines 10500a/b; Table 2; Figs.10b and 11). Secondary fractures, however, are strongly affected by variations in lithology and bedding, with nearly all secondary fractures terminating at the boundary between these two facies (Fig. 11), and an approximate three-fold increase in FI and extension is observed in the limestone bed relative to the sandstone bed (Table 2).

In the Frasnian reefal-slope and forereef in Windjana Gorge syndepositional fractures are variably developed, and are generally characterized by smaller apertures (<2 cm) and lower vertical relief (<10 m) than observed within age-equivalent platform strata. The sponge–stromatoporoid boundstone facies (scanline 9542; Table 2; Figs. 9 and 10c) which mantles the collapse scar in the "classic face" (Fig. 9; Playford et al., 1989), is dominated exclusively by closely-spaced, small syndepositional fractures ($b < 1$ cm) and displays modest extension values. Syndepositional fractures are abundant in the debris flow deposits of the Frasnian forereef slope (Table 2). Fractures in this setting are often restricted to individual debris flow beds, and commonly terminate into bedding-parallel fractures referred to by Playford (1984) as neptunian sills (Fig. 10d), which are interpreted to represent bedding-plane slip associated with down-slope creep of sediments deposited above the angle of repose.

Syndepositional fracture development in the Frasnian section appears to be strongly linked to two key parameters: (1) early-

marine cementation patterns and microbial binding, and (2) proximity to the platform-margin escarpment. In the Frasnian, marine cementation and microbial activity are strongest within a few hundreds of meters of the platform margin in the reef and reef-flat facies tracts, and diminish rapidly into proximal backreef and forereef strata (Kerans, 1985). Syndepositional fracture development tracks these early-lithification patterns, with the most deformation occurring near the platform margin, and generally decreases away from the platform margin as a function of decreasing early lithification (e.g., scanlines 9460 and 10500; Table 2; Fig. 9). The late Frasnian platforms of the Canning Basin typically developed a high-relief (30–100 m), sub-vertical platform-margin escarpment, which in many cases became over-steepened and prone to collapse (Fig. 9; Playford, 1980; Ward, 1996; George et al., 1997; Playton, 2008). Extensional stress associated with the gravitational instability of the unconfined escarpment is interpreted to be strongest proximal to the platform margin, and has been described in many modern platforms (Daugherty, 1986; Whitaker and Smart, 1997; Guidry et al., 2007).

6.2. Fracture patterns in Famennian facies

Within the exposures of prograding Famennian platform margin and upper forereef strata at the west entrance to Windjana Gorge, three depositional facies with distinct fracture patterns are differentiated (Fig. 12; Table 2): (1) massive, microbial boundstone; (2) laminar, microbial boundstone; and (3) bedded, sponge–microbial boundstone. Early-marine cementation and microbial binding are extensive in each of these facies, and in most cases, syndepositional fractures are vertically extensive (up to 100 m), with even modest aperture fractures ($b > 2.5$ cm) extending upwards for several tens of meters, crosscutting numerous bedding contacts (Figs. 4 and 5a).

The massive microbial boundstone facies consists of calcimicrobes, sponges, and platform-derived sediments (<30% Fig. 12a). Extensive early lithification of this facies is evidenced by significant microbial encrustation and large volumes of marine and micritic cement infilling growth cavities (Kerans, 1985; Hurley and Lohmann, 1989). The massive microbial boundstone is the most extensively fractured of all the Famennian facies sampled by this study, with syndepositional extension values of approximately 10% and large-aperture fractures (up to 64 cm) often occurring in clusters (Fig. 13; scanline 9559, Table 2). Fracture fills are highly variable, and consist of a mix of platform-derived material (ooid grainstone, skeletal debris, sandstone), and radiaxial fibrous marine cement, suggesting that fractures in this facies were well connected to the sea floor (Figs. 6c,e–f and 12a).

The laminar, microbial boundstone consists of lenses of sponge-rich microbial boundstone and variable amounts of platform-derived, terrigenous wackestone and packstone (Kerans, 1985; Figs. 12b,c and 14). Syndepositional fractures are well developed in this facies with extension values ranging from 8 to 9%, and apertures of up to 50 cm observed (e.g., scanlines 9447 and 9775, Table 2). Small-scale faults are also present in this facies, running subparallel to bedding with minor offset (<1m; Fig. 12b). Syndepositional fractures tend to occur in clusters in this facies, and appear to be largely unaffected by the lithologic contrast between the microbial lenses and the terrigenous wacke/packstone and in many cases extend upwards for several tens of meters (Fig. 14). However, as with the Frasnian backreef facies (Fig. 11), secondary fractures are strongly affected by the lithology contrasts within this facies, and are almost exclusively restricted to the microbial lenses (Fig. 14).

The bedded, sponge, microbial boundstone facies is composed of alternating steeply-dipping (30–35°) beds of sponges, receptaculitids (sponge-like organisms), binding and encrusting microbial organisms, marine cement, and platform-derived sediments

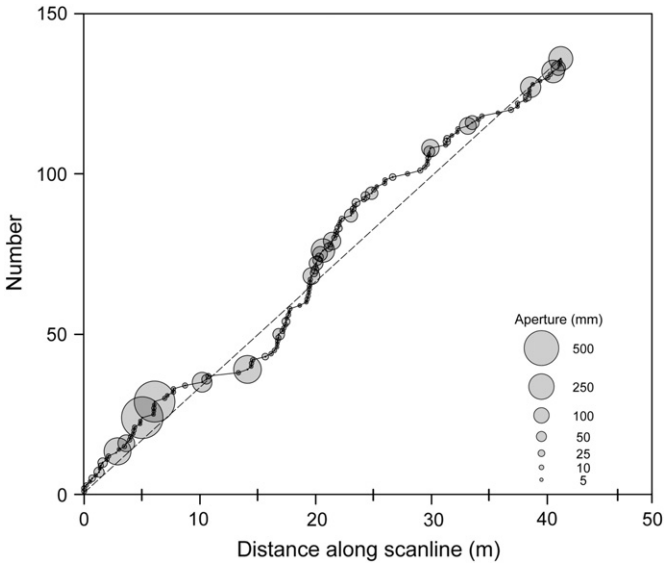

Fig. 13. Evidence of fracture clustering, scanline 9559, Famennian reef, Windjana Gorge. Cumulative fracture number is plotted against location along scanline. Where curve is steeper than the uniform distribution trend line (dashed line), fractures are clustered. Note clustering of large-aperture fractures, with the two of largest-aperture fractures occurring in close proximity to one another.

(Fig. 12d). This facies marks the transition between the reefal-slope and forereef, and based on geometric restorations was likely deposited in a water depth of approximately 100–150 m (Stephens and Sumner, 2003). Syndepositional fractures are well developed in this facies, with extension values ranging from 5 to 7%, and apertures ranging from 1 to 15 cm wide. Syndepositional fractures are typically lined with scalenohedral and radiaxial–fibrous cements, and platform-derived sediment fills are rare; implying an early-marine-burial origin (burial depths of a few tens of meters) and limited connection with the sea floor. Fractures in this facies are often linked by bedding-parallel, slip planes (Fig. 12d), which potentially help accommodate extension in the overlying strata.

7. Scales of mechanical units and temporal evolution of mechanical stratigraphy

Fracture patterns in carbonates are strongly influenced by the rigidity, thickness, and layering of mechanical units (Ladeira and Price, 1981; Corbett et al., 1987; Narr and Suppe, 1991; Bai and Pollard, 2000; Underwood et al., 2003; Shackleton et al., 2005; Ferrill and Morris, 2008). A mechanical layer has commonly been defined as a package of rock with the same general mechanical properties (i.e., rigidity), with fractures generally terminating at the unit's upper and lower interface. Mechanical layers in many cases do not correlate directly with stratigraphic horizons and may crosscut bedding planes and lithologic boundaries. The mechanical stratigraphy of a succession of rocks is characterized by (1) the thickness and rigidity of individual mechanical units, (2) the stacking of mechanical layers, and (3) the nature of the interface between mechanical layers. As outlined in the preceding sections syndepositional fractures in the Canning Basin are observed to crosscut multiple bed- to cycle-scale "apparent" mechanical units (0.25–5.0 m scale units; Figs. 9, 11, and 14). In contrast, post-depositional fracture patterns are strongly influenced by these small-scale mechanical layers (Figs. 11 and 14).

The data presented by this study demonstrate that while syndepositional fracture patterns are clearly influenced by depositional facies, lithologic heterogeneity associated with bedding and

high-frequency cycle boundaries (0.25–5.0 m scale units; Figs. 11 and 14) does not provide sufficient mechanical contrast to terminate syndepositional fractures. Instead, syndepositional mechanical unit differentiation depends on early-lithification patterns within a carbonate platform, with extensive syndepositional fracturing restricted to early-cemented zones. During syndepositional fracture development in the Canning Basin, the mechanical contrast between individual beds was low, with early-lithified strata effectively behaving as *one* mechanical unit, regardless of bedding or lithology (Fig. 15a). Moreover, fractures are effectively terminated only by large-scale rigidity contrasts associated with the transition between early-lithified facies and unlithified facies (e.g., reef to uncemented slope) or in some cases at sequence boundaries in the platform interior (Fig. 9). The relationship suggests that mechanical unit differentiation in early-fracture systems (prior to burial diagenesis) occurs at roughly the stratigraphic sequence scale to formation scale (25–200 m), with the transition between early-lithified unlithified strata defining early mechanical unit boundaries (Fig. 9).

Secondary fractures in the Devonian reef complexes are far more sensitive to small-scale mechanical heterogeneity, and typically terminate at bed-scale lithologic contrasts (Figs. 11 and 14). The observation that secondary fractures terminate at boundaries which syndepositional fractures originally crosscut suggests that the mechanical stratigraphy of the Devonian reef complexes have evolved over time. Differential diagenesis of individual facies associated with burial introduces increased mechanical heterogeneity, and various lithologies begin to develop unique mechanical properties (Fig. 15b). As a result, strata that initially behaved as one mechanical unit prior to burial become increasingly partitioned, and multiple mechanical layers develop, strongly affecting secondary fracture patterns (Fig. 15b).

Recent studies have shown that mechanical stratigraphy is not static; instead, mechanical properties are dynamic and fluid-flow along fracture networks and progressive diagenesis can have a pronounced effect on the temporal evolution of mechanical properties and subsequent fracture patterns (Marrett and Laubach, 2001; Shackleton et al., 2005; Laubach and Ward, 2006). Previous workers in the Canning Basin (Hurley, 1986; Kerans et al., 1986) have proposed that the early-fracture permeability system is responsible for enhancing early-marine cementation, effectively creating a feedback loop in which fracturing leads to enhanced early lithification throughout the platform, which in turn promotes increased fracturing.

Diagenetic events following early-fracture development in the Canning Basin served to introduce increasing mechanical heterogeneity into the system, with a shift from large-scale mechanical units to increasingly finer scale, and heterogeneous mechanical units. As a result, the mechanical stratigraphy and the subsequent vertical connectivity of a given fracture network is fundamentally linked to the timing of deformation relative to the diagenetic history of the system, and needs to be carefully considered.

8. Variations in fracture pattern as a function of stratigraphic architecture

When both outcrop and remote-sensing data are considered, a statistically significant relationship between fracture intensity (FI) and P/A ratio is observed in both the platform margin and platform interior of the Devonian reef complexes (Frost and Kerans, 2009; Fig. 16). FI increases linearly with P/A ratio, with an approximate two-fold increase in FI between the most progradational platforms (high P/A) relative to the most retrogradational platforms (negative P/A; Table 1). All platform-margin data points plot within the same 95% confidence interval (Fig. 16), regardless of control type and proximity to regional syndepositional tectonic elements (e.g., Scanline NO-SM; Fig. 8b). In the backreef, the relationship between FI and P/A ratio is observed only for gravitational and antecedent topography controlled systems (Fig. 16). Fracture populations controlled by active tectonic deformation consistently produce fracture intensities two to three times higher than predicted by relationship with P/A ratio, and plot well outside the 95% confidence interval for gravitational and antecedent topography controlled systems. Frost and Kerans (2009) suggest that the relationship between FI and P/A ratio is controlled by two key factors (Fig. 17): (1) the architecture and mechanical properties of the material that a platform builds over as it progrades, aggrades, or retrogrades; and (2) the impact that variations in stratigraphic architecture imparts on the relative efficiency of syndepositional fracture controls.

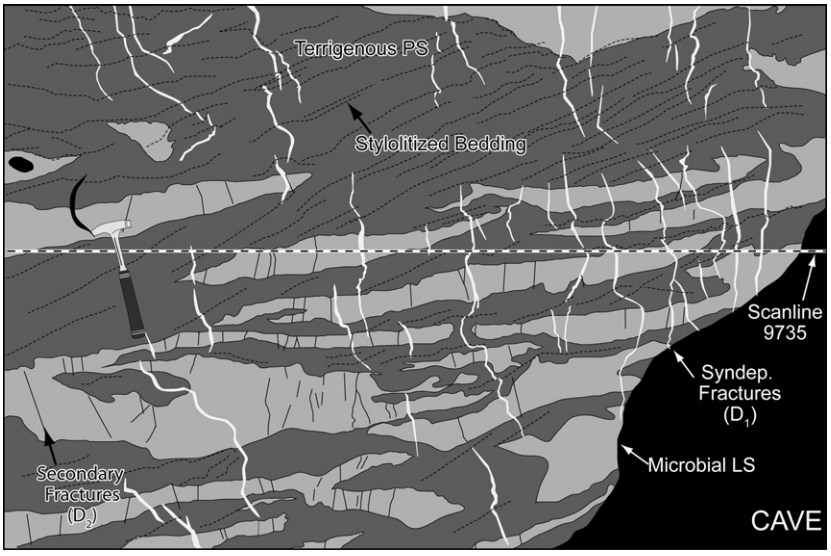

Fig. 14. Fracture patterns in laminar microbial boundstone, scanline 9735, Windjana Gorge (see Fig. 13c for reference). Syndepositional fractures are best developed in the microbial boundstone shelves and to a lesser degree in mixed detrital matrix sediment, while secondary fractures are largely restricted to the microbial lenses. Early fractures are folded and crosscut by dissolution seams and stylolites in the detrital matrix.

During progradation, early-cemented and brittle platform-margin facies grow basinward over unstable and ductile forereef and compactable basinal strata. Under these conditions fracture development is driven by stress generated from gravitational controls including mechanical compaction of unconsolidated slope and basinal strata, bedding-plane slippage in the slope, and platform-margin instability. Mechanical compaction values as high as 70% have been reported for basinal sediments in the Canning Basin (Playford, 1984; Playford and Wallace, 2001), and Goldhammer (1997) showed that mechanical compaction of carbonate muds can occur during early burial and at very shallow depths (e.g., 50% porosity reduction within 100 m of burial). The portion of the carbonate platform that is subjected to deformation by these processes is largely governed by the distance that a platform progrades beyond the previous platform margin, and is referred to as the zone of enhanced syndepositional deformation (EDz, Frost and Kerans, 2009; Fig. 17). With increasing P/A ratios (flatter platform-margin trajectory), progressively larger amounts of slope and basinal strata are loaded and subsequently compacted, creating a progressively wider zone of enhanced syndepositional deformation and leading to increased fracturing (Fig. 17).

In aggrading or retrograding margins, where younger platforms build upward, or retreat landward, over older early-lithified platform-margin or platform-interior strata, fracturing in the platform-margin facies is dominantly driven by stresses associated with gravitational instability of the platform-margin related to over-steepening and collapse (Fig. 17). Under these conditions, fracturing is related to escarpment height, and consequently is strongest in high-rising aggradational platforms (>100 m tall), and diminishes in lower-relief retrograding platforms. Moreover, the efficiency of gravitational controls on fracture development in aggrading or retrograding diminishes into the platform interior, and as a result, the zone of enhanced syndepositional deformation is restricted to a small swath near the platform margin (Fig. 17). As a result, syndepositional fractures are weakly developed in the platform interior in the absence of external controls (e.g., regional tectonic deformation). Fracturing under these conditions depends on differential compaction over rigid antecedent topography and/or syndepositional faulting, with highs in fracture intensity occurring near faults (e.g., scanline SO_Fr-7; Fig. 8a) or over basement highs (e.g., scanline SO_FR-6; Fig. 8a).

9. Comparison to other settings, and implications for styles of early deformation

The syndepositional fracture patterns observed in the Canning Basin display many similarities to other high-relief carbonate platforms, as well as several key differences. The most obvious

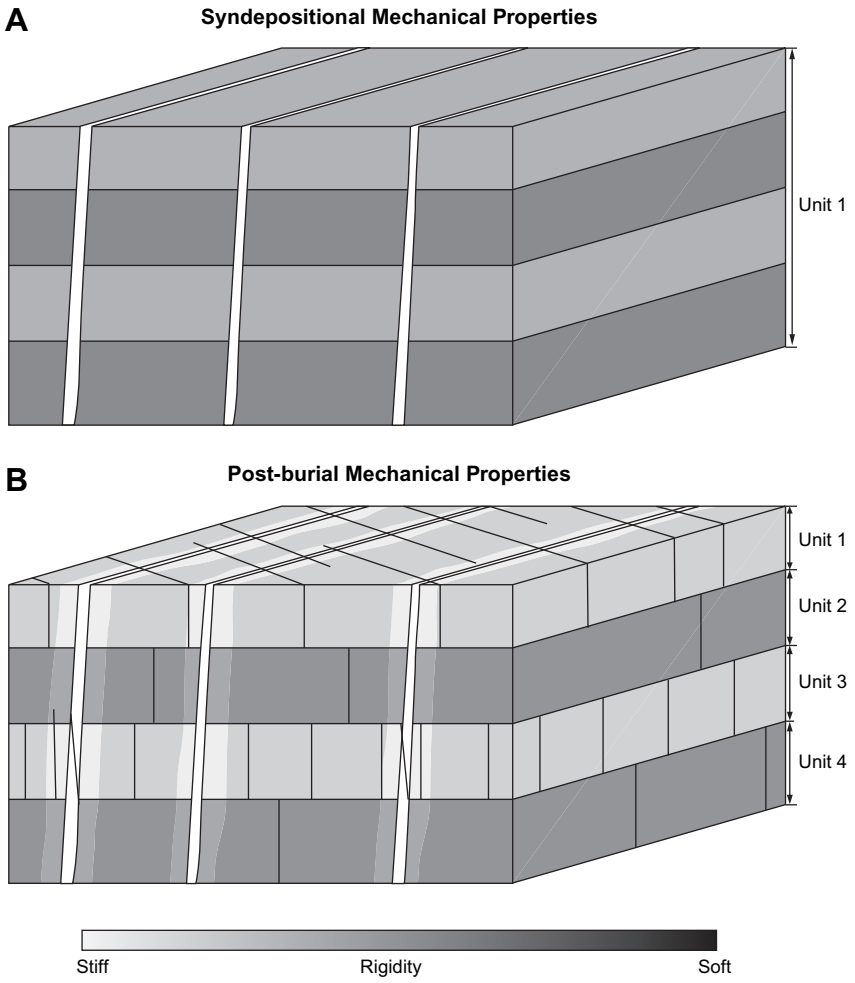

Fig. 15. Fracture patterns related to mechanical property evolution. (A) During syndepositional fracture development, all layers are rigid enough for fractures to propagate; however, rigidity contrasts at bedding boundaries are insufficient to terminate fractures. Fractures crosscut all layers, with all beds effectively behaving as one mechanical unit. (B) Following burial diagenesis, the mechanical contrast between individual beds increases, effectively creating four mechanical units with secondary fractures confined within each of these layers.

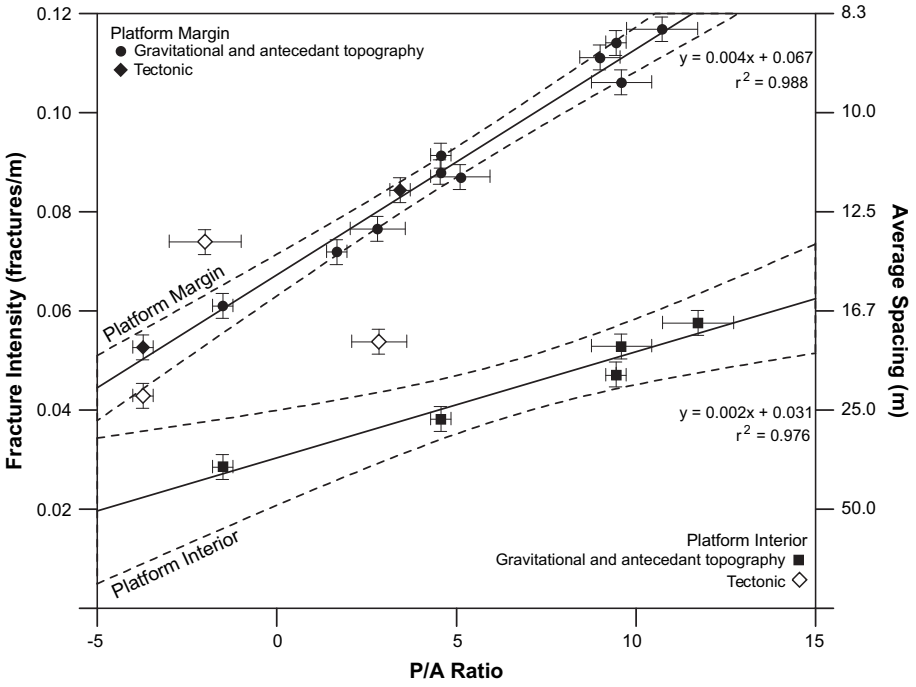

Fig. 16. Normalized fracture intensity (FIn) for fractures with apertures greater than 0.5 m as a function of progradation/aggradation (P/A) ratio (modified from Frost and Kerans, 2009). Platform-margin (upper curve) and backreef facies (lower curve) plotted with a linear regression and 95% confidence intervals. Data from structurally controlled settings (e.g., Southern Oscar Range, Tunnel Creek) not included in platform-interior regression. Horizontal error bars represent uncertainty in calculating P/A ratio, while vertical error bars represent uncertainty in calculating fracture intensity.

comparison is to the Permian-age Capitan System of Texas and New Mexico, which is characterized by prograding and aggrading, high-relief, early-lithified, carbonate platforms (Kerans and Tinker, 1999). Syndepositional deformation in these strongly progradational platforms (P/A ratio of 7–25; Osleger, 1998; Kerans and Tinker, 1999) has been described by Hunt and Fitchen (1999), Hunt et al. (2002), Kosa et al. (2003), and Kosa and Hunt (2005, 2006), and numerically modeled by Resor and Flodin (this issue).

Syndepositional growth faulting is the dominant style of deformation in the Capitan platform interior, with opening-mode fractures being generally restricted to the platform margin (Kosa and Hunt, 2005). Deformation in the Capitan System has generally been attributed to compaction of basinal and slope strata (Hunt and Fitchen, 1999; Hunt et al., 2002; Resor and Flodin, this issue). By comparison, compaction-related growth faulting is rare in the Canning Basin and is restricted to the platform interior of the most progradational platforms (e.g., Billy Munro Gorge, P/A ≈ 11). There are two possible explanations for the differing styles of deformation in these settings. (1) The mechanical properties (degree of early lithification) of the Capitan System favor growth faulting rather than fracturing, or (2) the style of deformation is controlled by P/A ratio — namely, that stress associated with increased vertical

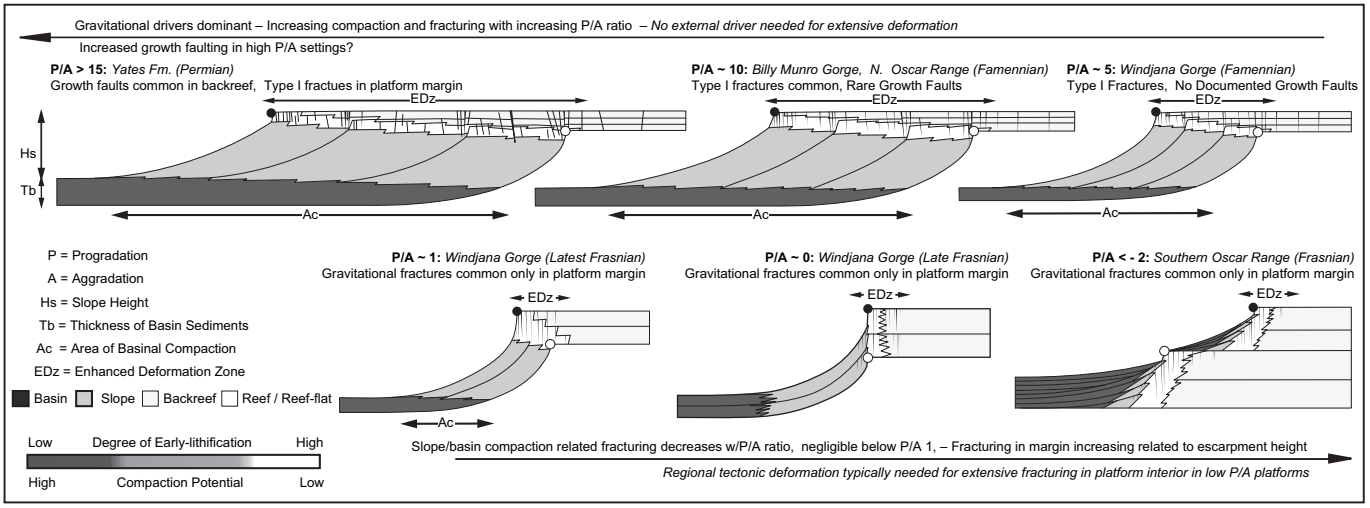

Fig. 17. Basis for the relationship between P/A ratio and syndepositional fracture patterns (Modified from Frost and Kerans, 2009). In prograding platforms, increasing amounts of slope and basinal strata are loaded, leading to increasing compaction, bedding-plane slippage, and subsequently more fracturing. In the most progradational platforms growth faulting becomes increasingly common (e.g., Yates Formation, Billy Munro Gorge). In aggrading and retrograding platforms, compaction of slope and basinal strata is far less important. Here, gravitational instability of the escarpment drives fracturing in the platform margin, while external drivers are required for extensive fracturing in the backreef.

displacement from higher amounts of basinal compaction in high P/A platforms is accommodated by growth faults rather than by purely opening-mode fractures as in low P/A platforms.

Early-marine cementation is prevalent in both the Devonian reef complexes (Playford, 1980; Kerans, 1985) and the Capitan Formation (Kirkland-George et al., 1993), and syndepositional fractures are generally well developed in early-lithified zones of both systems. In both localities the presence or absence of early-marine lithification clearly acts as a control on the distribution of syndepositional fractures; however no evidence has been presented to suggest that this parameter alone governs the style of early deformation (faulting versus fracturing).

In the Capitan System, Kosa and Hunt (2005) report that growth faults often develop along preexisting syndepositional fractures in older reef strata due to vertical displacement associated with basinal compaction. Numerical modeling conducted by Resor and Flodin (this issue) demonstrates that compaction-related vertical displacement in the platform margin and outer shelf increases with both P/A ratio and continued burial associated with platform growth. Given these observations, it seems plausible that fractures which originated as opening-mode, begin to develop a sense of shear due to increased vertical displacement associated with both progradation and continued burial. When the observations from the Capitan System (Kosa and Hunt, 2005; Resor and Flodin, this issue) are considered with the findings of this study it appears that P/A ratio exerts a strong control on the transition from fracturing to growth faulting as the dominant style of early deformation, with the most progradational platforms being fault-dominated, and lower P/A platforms (P/A < 5) fracture-dominated (Fig. 17).

10. Conclusions

Fracture patterns and mechanical stratigraphy are dynamic, time-sensitive variables. Syndepositional fracture patterns are strongly affected by position relative to the platform margin, depositional setting, and facies, with the degree of early lithification playing an important role in fracture development. The strong relationship between fracture intensity and progradation/aggradation ratio demonstrated here implies that stratigraphic architecture is a fundamental and intrinsic control on syndepositional deformation in carbonate platforms, and implies external drivers are not required for extensive syndepositional deformation. Recognizing that significant deformation can occur in carbonate platforms prior to burial and in the absence of regional tectonic activity is critical to accurately predicting reservoir properties in carbonate systems. By relating syndepositional deformation to observable criteria such as platform-margin trajectory (progradation/aggradation ratio), lithofacies, depositional environment and tectonic setting, the results presented here take a significant step toward developing predictive relationships between syndepositional fracture development and stratigraphic architecture in the subsurface using seismic or well data.

Acknowledgements

We extend warm thanks to the following for their invaluable help with this project: Philip Playford and Roger Hocking of the Geologic Survey of Western Australia, Chris Zahm (RCRL), Wayne Narr and Eric Flodin (Chevron), Dan Carpenter, Jim DeGraff, and Jim Anderson (ExxonMobil), Phil Resor (Wesleyan University), Eduard Kosa (Shell), and my field assistants Annie Frost and Steve Rogers. Satellite imagery was graciously provided by ExxonMobil Upstream Research. Field and logistical support were provided by the Geological Survey of Western Australia. This research was funded in part by the Jackson School of Geosciences Foundation, the Bureau of Economic Geology's Reservoir Characterization Research Laboratory, ConocoPhillips, Chevron, GSA, and the AAPG Foundation. Publication authorized by the Director, Bureau of Economic Geology.

References

Baceta, J.I., Wright, V.P., Beavington-Penney, S.J., Pujalte, V., 2007. Palaeohydrogeological control of paleokarst macro-porosity genesis during a major sea-level lowstand: Danian of the Urbasa-Andia plateau, Navarra, North Spain. Sedimentary Geology 199, 141.

Bai, T., Pollard, D.D., 2000. Fracture spacing in layered rocks: a new explanation based on the stress transition. Journal of Structural Geology 22, 43–57.

Bathurst, R.G.C., 1982. Genesis of stromatactis cavities between submarine crusts in Paleozoic carbonate mud buildups. Journal of the Geological Society of London 139, 165–181.

Brown, S.A., Boserio., I.M., Jackson, K.S., Spence, K.W., 1984. The geological evolution of the Canning Basin; implications for petroleum exploration, In: Purcell, P.G. (Ed.), The Canning Basin W.A. Proceedings of the Geological Society of Australia/Petroleum Exploration Society of Australia Canning Basin Symposium, Perth, WA, pp. 85–96.

Chow, N., George, A.D., Trinajstic, K.M., 2004. Tectonic control on development of a Frasnian–Famennian (Late-Devonian) paleokarst surface, Canning Basin reef complexes, northwestern Australia. Australian Journal of Earth Sciences 51, 911–917.

Collins, J.F., Kenter, J.A.M., Harris, P.M., Kuanysheva, G., Fischer, D.J., Steffen, K.L., 2006. Facies and Reservoir-quality variations in the Late Visean to Bashkirian outer platform, rim, and flank of the Tengiz Buildup, Precaspian Basin, Kazakhstan. In: Harris, P.M., Weber, L.J. (Eds.), Giant Hydrocarbon Reservoirs of the World: From Rocks to Reservoir Characterization and Modeling, 88. American Association of Petroleum Geologists Memoir, pp. 55–95.

Corbett, K.P., Friedman, M., Spang, J., 1987. Fracture development and mechanical stratigraphy of Austin Chalk, Texas. AAPG Bulletin 71, 17–28.

Cozzi, A., 2000. Synsedimentary tensional features in Upper Triassic shallow-water platform carbonates of the Carnian Prealps (northern Italy) and their importance as palaeostress indicators. Basin Research 12, 133–146.

Craig, J.D., Downey, J.W., Gibbs, A.D., Russell, J.R., 1984. The application of Landsat imagery in structural interpretation of the Canning Basin, W.A., In: Purcell, P.G., (Ed.), The Canning Basin W.A. Proceedings of the Geological Society of Australia/Petroleum Exploration Society of Australia Canning Basin Symposium, Perth WA, pp. 57–71.

Daugherty, D.R., 1986. Characteristics and origins of joints and sedimentary dikes of the Bahama Islands, In: Boardman, M.R. Metzler, C.V. (Eds.), Proceedings of the Symposium on the Geology of the Bahamas 3, 45–56.

Della Porta, G., Kenter, J.A.M., Bahamonde, J.R., 2004. Depositional facies and stratal geometry of an Upper Carboniferous prograding and aggrading high-relief carbonate platform (Cantabrian Mountains, N. Spain). Sedimentology 51, 267–295.

Doglioni, C., Goldhammer, R.K., 1988. Compaction-induced subsidence in the margin of a carbonate platform. Basin Research 1, 237–246.

Dörling, S.L., Dentith, M.C., Groves, D.I., Playford, P.E., Vearncombe, J.R., Muhling, P., Windrim, D., 1996. Heterogeneous brittle deformation in the Devonian carbonate rocks of the Pillara Range, Canning Basin: implications for the structural evolution of the Lennard Shelf. Australian Journal of Earth Sciences 43, 15–30.

Drummond, B.J., Etheridge, M.A., Davies, P.J., Middleton, M.F., 1988. Half-graben model for the structural evolution of the Fitzroy Trough, Canning Basin, and implications for resource exploration. APEA Journal 28, 76–86.

Eyles, N., Eyles, C.H., Apak, S.N., Carlsen, G.M., 2001. Permian–Carboniferous tectono-stratigraphic evolution and petroleum potential of the northern Canning Basin, Western Australia. AAPG Bulletin 85, 989–1006.

Ferrill, D.A., Morris, A.P., 2008. Fault zone deformation controlled by carbonate mechanical stratigraphy, Balcones fault system. Texas. AAPG Bulletin 92, 359–380.

Fischer, A.G., 1964. The lofer cyclothems of the Alpine Triassic. Kansas Geological Survey Bulletin 1, 107–149.

Frost, E.L., 2007. Facies heterogeneity, platform architecture and fracture patterns of the Devonian reef complexes. PhD thesis, The University of Texas at Austin.

Frost, E.L., Kerans, C., 2009. Platform-margin trajectory as a control on Syndepositional fracture Patterns, Canning Basin, Western Australia. Journal of Sedimentary Research 79, 44–55.

George, A.D., Playford, P.E., Powell, C.M., Tornatora, P.M., 1997. Lithofacies and sequence development on an Upper Devonian mixed carbonate–siliciclastic fore-reef slope, Canning Basin, Western Australia. Sedimentology 44, 843–867.

Ginsburg, R.N., James, N.P., 1976. Submarine botryoidal aragonite in Holocene reef limestones, Belize. Geology 4, 431–436.

Goldhammer, R.K., 1997. Compaction and decompaction algorithms for sedimentary carbonates. Journal of Sedimentary Research 67, 26–35.

Grammer, M.G., Ginsburg, R.N., Swart, P.K., McNeill, D.F., Timothy Jull, A.J., Prezbindowski, D.R., 1993. Rapid growth rates of syndepositional marine aragonite cements in steep marginal slope deposits, Bahamas and Belize. Journal of Sedimentary Petrology 63, 983–989.

Grammer, G.M., Crescini, C.M., McNeill, D.F., Taylor, L.H., 1999. Quantifying rates of syndepositional marine cemetation in deeper platform environments – new insight into a fundamental process. Journal of Sedimentary Research 69, 202–207.

Guidry, S.A., Grasmueck, M., Carpenter, D.G., Gombos Jr., A.M., Bachtel, S.L., Viggiano, D.A., 2007. Karst and early-fracture networks in carbonates, Turks and Caicos Islands, British West Indies. Journal of Sedimentary Research 77, 508–524.

Harris, P.M., Kendall, C.G.S.T.C., Lerche, I., 1985. Carbonate cementation: a brief review. In: Schneidermann, J.S., Harris, P.M. (Eds.), Carbonate Cements, vol. 36. Society of Economic Paleontologists and Mineralogists, Special Publication, pp. 79–95.

Hunt, D.W., Fitchen, W.M., 1999. Compaction and the dynamics of carbonate-platform development; insights from the Permian Delaware and Midland basins; southeastern New Mexico and West Texas, U.S.A. In: Harris, P.M., Saller, A.H., Simo, J.A. (Eds.), Advances in Carbonate Sequence Stratigraphy; Application to Reservoirs, Outcrops and Models, vol. 63. Society of Economic Paleontologists and Mineralogists, Special Publication, pp. 75–106.

Hunt, D.W., Fitchen, W.M., Kosa, E., 2002. Syndepositional deformation of the Permian Capitan reef carbonate platform, Guadalupe Mountains, New Mexico, USA. Sedimentary Geology 154, 89–126.

Hurley, N.F., 1986. Geology of the Oscar Range Devonian Reef Complex, Canning Basin, Western Australia. PhD thesis, University of Michigan, Ann Arbor.

Hurley, N.F., Lohmann, K.C., 1989. Diagenesis of Devonian reefal carbonates in the Oscar Range, Canning Basin, Western Australia. Journal of Sedimentary Petrology 59, 127–146.

James, N.P., Ginsburg, R.N., 1979. The seaward marginal Belize barrier and atoll reefs. International Association of Sedimentologists Special Publication, 3, 191 p.

James, N.P., Ginsburg, R.N., Marszalek, D.S., Choquette, P.W., 1976. Facies and fabric specificity of early subsea cements in shallow Belize (British Honduras) reefs. Journal of Sedimentary Petrology 46, 523–544.

Jones, G.D., Xiao, Y., 2006. Geothermal convection in the Tengiz carbonate platform, Kazakhstan: reactive transport models of diagenesis and reservoir quality. American Association of Petroleum Geologists Bulletin 90, 1251–1272.

Kerans, C., 1985. Petrology of Devonian and Carboniferous carbonates of the Canning and Bonaparte Basins. Western Australian Mining and Petroleum Research Institute, Report 12.

Kerans, C., Tinker, S.W., 1999. Extrinsic stratigraphic controls on development of the Capitan Reef Complex. In: Saller, A.H., Harris, P.M., Kirkland, B.L., Mazzullo, S.J. (Eds.), Geological Framework of the Capitan Reef, vol. 65. Society of Economic Paleontologists and Mineralogists, Special Publication, pp. 15–36.

Kerans, C., Hurley, N.F., Playford, P.E., 1986. Marine diagenesis in Devonian reef complexes of the Canning Basin, Western Australia. In: Schroeder, J.H., Purser, B.H. (Eds.), Reef Diagenesis. Springer-Verlag, Berlin, pp. 357–380.

Kirkland-George, B.L., Longacre, S.A., Stoudt, E.L., 1993. Reef. In: Bebout, D.G., Kerans, C. (Eds.), Guide to the Permian Reef Geology Trail, McKittrick Canyon, Guadalupe Mountains National Park, 26. Bureau of Economic Geology Guidebook, West Texas, pp. 23–31.

Kosa, E., Hunt, D.W., 2005. Growth of syndepositional faults in carbonate strata; Upper Permian Capitan Platform, New Mexico, USA. Journal of Structural Geology 27, 1069–1094.

Kosa, E., Hunt, D.W., 2006. Heterogeneity in fill and properties of karst-modified syndepositional faults and fractures: Upper Permian Capitan platform, New Mexico, U.S.A. Journal of Sedimentary Research 76, 131–151.

Kosa, E., Hunt, D.W., Fitchen, W.M., Bockel-Rebelle, M., Roberts, G., 2003. The heterogeneity of paleocavern systems developed along syndepositional fault zones; the Upper Permian Capitan Platform, Guadalupe Mountains, U.S.A. In: Ahr, W.M., Harris, P.M., Morgan, W.A., Somerville, I.D. (Eds.), Permo-Carboniferous Carbonate Platforms and Reefs, vol. 78. Society of Economic Paleontologists and Mineralogists, Special Publication, pp. 291–322.

Ladeira, F.L., Price, N.J., 1981. Relationship between fracture spacing and bed thickness. Journal of Structural Geology 3, 179–183.

Land, L.S., Moore, C.H., 1977. Deep forereef and upper island slope, north Jamaica. American Association of Petroleum Geologists Studies in Geology 4, 53–65.

Land, L.S., Moore, C.H., 1980. Lithification, micritization, and syndepositional diagenesis of biolithites on the Jamaican Island slope. Journal of Sedimentary Petrology 50, 357–370.

Laubach, S.E., Ward, M.E., 2006. Diagenesis in porosity evolution of opening-mode fractures, Middle Triassic to Lower Jurassic La Boca Formation, NE Mexico. Tectonophysics 419, p. 75.

Marrett, R., Laubach, S.E., 2001. Fracturing during Burial Diagenesis. University of Texas at Austin, 28. Bureau of Economic Geology, Guidebook, pp. 109–123.

Marrett, R., Ortega, O.J., Kelsey, C.M., 1999. Extent of power-law scaling for natural fractures in rock. Geology 27, 799–802.

Melim, L.A., Scholle, P.A., 2002. Dolomitization of the Capitan Formation forereef facies (Permian, west Texas and New Mexico): see page reflux revisited. Sedimentology 49, 1207–1227.

Miller, J.M., Nelson, E.P., Hitzman, M., Muccilli, P., Hall, W.D.M., 2007. Orthorhombic fault-fracture patterns and non-plane strain in a synthetic transfer zone during rifting: Lennard shelf, Canning basin, Western Australia. Journal of Structural Geology 29, 1002–1021.

Narr, W., Suppe, J., 1991. Joint spacing in sedimentary rocks. Journal of Structural Geology 13, 1037–1048.

Nelson, R.A., 1985. Geologic analysis of naturally fractured reservoirs. In: Contributions in Petroleum Geology and Engineering. 1 Gulf Publishing Co., Houston.

Ortega, O.J., Marrett, R.A., Laubach, S.E., 2006. A scale-independent approach to fracture intensity and average spacing measurement. AAPG Bulletin 90, 193–208.

Osleger, D.A., 1998. Sequence architecture and sea-level dynamics of Upper Permian shelfal facies, Guadalupe Mountains, southern New Mexico. Journal of Sedimentary Research 68, 327–346.

Playford, P.E., 1980. Devonian "Great Barrier Reef" of Canning Basin, Western Australia. The American Association of Petroleum Geologists Bulletin 64, 814–840.

Playford, P.E., 1984. Platform-margin and marginal-slope relationships in Devonian reef complexes of the Canning Basin, in: Purcell, P.G., (Ed.), The Canning Basin W.A. Proceedings of the Geological Society of Australia/Petroleum Exploration Society of Australia Canning Basin Symposium, Perth WA, pp. 189–214.

Playford, P.E., 2002, Paleokarst, pseudokarst, and sequence stratigraphy in Devonian reef complexes of the Canning Basin, Western Australia, in: Keep, M., Moss, S.J. (Eds.), The Sedimentary Basins of Australia. Proceedings of the Petroleum Exploration Society of Australia 3, pp. 763–793.

Playford, P.E., Hocking, R., 1999. Devonian reef complexes of the Canning Basin. Geological Survey of Western Australia Bulletin 145, plates, 1–7.

Playford, P.E., Wallace, M.W., 2001. Exhalative mineralization in Devonian reef complexes of the Canning Basin, Western Australia. Economic Geology 96, 1595–1610.

Playford, P.E., Hurley, N.F., Kerans, C., Middleton, M.F., 1989. Reefal platform development, Devonian of the Canning Basin, Western Australia. In: Crevello, P.D., Wilson, J.L., Sarg, J.F., Read, J.F. (Eds.), Controls on Carbonate Platform and Basin Development, vol. 4. Society of Economic Paleontologists and Mineralogists, Special Publication, pp. 187–202.

Playton, T.E., 2008. Depositional elements, variations, and controls for reefal carbonate foreslope systems. PhD thesis, The University of Texas at Austin.

Price, N.J., 1966. Fault and Joint Development in Brittle and Semi-brittle Rock. Pergamon Press, Oxford.

Purser, B.H., 1971. Syn-sedimentary marine lithification of Middle Jurassic limestones in the Paris Basin. Sedimentology 12, 205–230.

Resor, P.G., Flodin, E.A.,. Forward modeling of synsedimentary deformation associated with a prograding steep rimmed carbonate margin. Journal of Structural Geology, this issue.

Rusciadelli, G., Di Simone, S., 2007. Differential compaction as a control on depositional architectures across the Maiella carbonate platform-margin (central Apennines, Italy). Sedimentary Geology 196, 133–155.

Schroder, J.H., 1973. Submarine and vadose cements in Pleistocene Bermuda reef rock. Sedimentary Geology 10, 179–204.

Shackleton, J.R., Cooke, M.L., Sussman, A.J., 2005. Evidence for temporally changing mechanical stratigraphy and effects on joint-network architecture. Geology 33, 101–104.

Shaw, R.D., Sexton, M.J., Zeilinger, I., 1995. The tectonic framework of the Canning Basin, WA, including 1:2 million structural elements map of the Canning Basin. Record 48, Australian Geological Survey Organization.

Shinn, E.A., 1969. Submarine lithification of Holocene sediments in the Persian Gulf. Sedimentology 12, 109–144.

Smart, P.L., Palmer, R.J., Whitaker, F., Wright, V.P., 1988. Neptunian dikes and fissure fills an overview and account of some modern examples. In: James, N.P., Coquette, P.W. (Eds.), Paleokarst. Springer-Verlag, New York, pp. 149–163.

Stephens, N.P., Sumner, D.Y., 2003. Famennian microbial reef facies, Napier and Oscar Ranges, Canning Basin, Western Australia. Sedimentology 50, 1283–1302.

Tinker, S.W., 1998. Shelf-to-basin facies distributions and sequence stratigraphy of a steep-rimmed carbonate margin; Capitan depositional system, McKittrick Canyon, New Mexico and Texas. Journal of Sedimentary Research 68, 1146–1174.

Underwood, C.A., Cooke, M.L., Simo, J.A., Muldoon, M.A., 2003. Stratigraphic controls on vertical fracture patterns in Silurian dolomite, northeastern Wisconsin. AAPG Bulletin 87, 121–142.

Wallace, M.W., Kerans, C., Playford, P.E., McManus, A., 1991. Burial diagenesis in the Upper Devonian reef complexes of the Geikie Gorge region, Canning Basin, Western Australia. American Association of Petroleum Geologists Bulletin 75, 1018–1038.

Ward, W.B., 1996. Platform evolution and diagenesis of Frasnian carbonate platforms, Devonian reef complexes, Napier Range, Canning Basin, Western Australia. PhD thesis, State University of New York at Stony Brook.

Whitaker, F.F., Smart, P.L., 1997. Groundwater circulation in a karstified bank marginal fracture system, South Andros Island, Bahamas. Journal of Hydrology 197.